# UCLA
## UCLA Electronic Theses and Dissertations

**Title**

Assessing the Aerosol Direct, Semi-Direct and Indirect Effects using Global Circulation Model Simulation Results

**Permalink**

https://escholarship.org/uc/item/5g44d8bm

**Author**

Huang, Huilin

**Publication Date**

2017

Peer reviewed|Thesis/dissertation

UNIVERSITY OF CALIFORNIA

Los Angeles

Assessing the Aerosol Direct, Semi-Direct and Indirect Effects

using Global Circulation Model Simulation Results

A thesis submitted in partial satisfaction

of the requirements for the degree Master of Arts

in Geography

by

Huilin Huang

2017

ABSTRACT OF THE THESIS

Assessing the Aerosol Direct, Semi-Direct and Indirect Effects using

Global Circulation Model Simulation Results

by

Huilin Huang

Master of Arts in Geography

University of California, Los Angeles, 2017

Professor Yongkang Xue, Chair

Aerosols come from both natural and anthropogenic sources and contribute large uncertainties to estimates of the Earth's changing energy budget. It is thus of great importance to understand the mechanism through which aerosols play a role on global climate. In this thesis, we investigate the direct and indirect effect of aerosols on global and regional climate variability (e.g. West Africa, South Asia and East Asia) using an atmospheric general circulation model, GFS (Global Forecast System) coupled with SSiB2 (the second version of Simplified Simple Biosphere Model). The three-dimensional aerosol data from the Goddard Chemistry Aerosol Radiation and Transport (GOCART) model has been adopted in this study.

We first analyze the direct effect of aerosols, especially absorption aerosols, on global and regional energy budget, precipitation, and surface temperature and the mechanism involved. For instance, we find the dust aerosol in North Africa produces a heating in the atmosphere, which

generates a cyclonic circulation in middle layer over Sahel region, which further brings about upward motion in the lower level and results in precipitation increase by 0.96 mm/day in June-July-August.

We also examine the impact of aerosols on ice clouds effective radius by applying an advanced ice cloud parameterization in the GCM. We find that increased aerosol loading reduces ice crystal size due to aerosol first indirect effect, with the maxima occurs in South Asia and North Indian Ocean. Ice clouds with smaller crystal sizes can absorb both shortwave and longwave radiation, thus resulting in less downward solar flux and less outgoing longwave on top of atmosphere (TOA). Global mean net radiation change on TOA is about $0.5 W/m^2$ and its sign is largely dependent on the relative magnitude of shortwave and longwave change and precipitation changes primarily respond to cooling/warming of the atmosphere.

Lastly, we use sulfate data in both pre-industrial and present-day case to test the impact of aerosols on liquid cloud effective radius. We find aerosols can act as cloud condensation nuclei, and hence change the shortwave optical properties of liquid clouds. Radiative cooling occurs globally because smaller droplets size leads to increased cloud albedo. The mean value is about $2.5 W/m^2$. Moreover, most radiative cooling occurs in North Hemisphere, where anthropogenic sulfate aerosols locate, such as East Asia and North America.

We also compare the radiative forcing of aerosol direct and indirect effect on both ice clouds and liquid clouds on global as well as the three monsoon regions. All aerosol effects result in radiative cooling on global scale. However, surface net radiation changes are different in West Africa, East and South Asia, which relates to local atmospheric conditions such as cloud cover and convection. Aerosol direct effect and aerosol indirect effect for liquid clouds have comparable impact on surface net radiation change (more than -3 $W/m^2$), while aerosol indirect effects for ice

cloud are smaller (~1 W/m$^2$) because of the negative feedback from cloud cover. Decreased land surface temperature can be found over North Hemisphere continent in all three effects, especially over higher latitude, with varied magnitude. The precipitation changes are less predictable. Aerosol indirect effects on averaged global precipitations are close to zero because the precipitation changes are different or even opposite in different regions. The effect of aerosol on precipitations can be influenced by convection strength, topography, and even the relative location of aerosols and monsoon system.

This thesis of Huilin Huang is approved.

Dennis P. Lettenmaier

Thomas W. Gillespie

Yongkang Xue, Committee Chair

University of California, Los Angeles

2017

# DEDICATION

to my family, and my dear friends

# Contents

# ACKNOWLEDGEMENTS

I would like to express my deepest thanks to my advisor, Professor Yongkang Xue, for his insightful guidance, tremendous help and constructive criticism from the beginning of my master study. I could not imagine I can finish this work without his support along the way.

I would express my gratitude to my committee member, Proferssor Dennis Lettenmaier and Professor Thomas Gillespie, for their constructive commentents on my work. And I also appreciate Proferssor Dennis Lettenmaier for recommending me in the transition from master to Ph.D. student.

I also appreciate all my coauthor. First, I would like to thank Dr. Yu Gu for her full support and creative advice to this work. I also thank Dr. Jonathan Jiang and Dr. Sarah Lu for helping me check the simulation results, and Dr. Mian Chin and Dr. Chun Zhao for offering the data. I would like to extend my appreciation to my fellow group, Dr. Ye Liu, Dr. Ismaila Diallo, Dr. Nagaraju Chilukoti, Dr. Qian Li, Dr. Bo Qiu, Dr. Wenkai Li, Jiping Quan for all the helpful discussion.

Finally, I would like to thank my family, my mother, father, grandmother and grandfather, and my dear friends. I would not be here without their unconditional love amd wholehearted support.

# Chapter 1

## 1. Background and overview

Atmospheric aerosols come from a wide variety of natural and anthropogenic sources. Natural aerosols such as dust are mostly associated with arid regions. Natural dust aerosols associated with arid regions such as North Africa, Middle East are hardly influenced by human activities. Another major natural aerosol source is the volcanic eruption, which could greatly enhance the sulfate aerosol concentrations in the stratosphere according to the Intergovernmental Panel on Climate Change (IPCC AR2) (1996). Anthropogenic aerosols include sulfate, nitrate, organic carbon (OC), and black carbon (BC), resulting from intensive human activities such as fossil fuel burning and land use changes (Zhang et al. 2012). Particularly, industrial sulfate aerosols and BC aerosols from the incomplete combustion of hydrocarbons have been increasing rapidly in Asia (Li et al. 2016). Aerosol particles have a lifetime of at most a few weeks in the troposphere and their distributions are highly inhomogeneous. The geographically localized sources and sinks and the relatively short atmospheric lifetimes give aerosols an extreme spatial and temporal inhomogeneity in the atmosphere (Haywood and Boucher 2000). Aerosols may undergo complex chemical reactions in the atmosphere and mix with each other before impacting on the surface (dry deposition) or being rained out (wet deposition) (Haywood and Boucher 2000)

Different types of aerosols may have very different effects on climate. Generally, aerosols affect global and regional climate through the scattering and/or the absorption of solar radiation (direct effect) (Figure. 1). Absorption aerosols such as dust and black carbon (BC) can also exert their influences on cloud water content and cloud cover due to the heating of the air column, called semi-direct effect (SDE). Aerosol direct effect is always accompanied by SDE. Located

1

interstitially in cloud droplets, absorption aerosols warm up the atmosphere, reduce the ambient relative umidity (RH) and suppress convective overturning, leading to the burn-off of clouds and reducing the planetary albedo (Hansen et al. 1997, Ackerman et al. 2000).

Aerosols also change cloud droplets number, effective radius (Re), and cloud water content, called aerosol indirect effect. The aerosol indirect effect is usually split into two effects: the first indirect effect, whereby an increase in aerosol concentration causes an increase in droplet number and a decrease in droplet size for a fixed liquid water content (Twomey 1974), and the second indirect effect, whereby the reduction in cloud droplet size affects the precipitation efficiency, tending to increase the liquid water content, the cloud lifetime (Albrecht 1989), and the cloud thickness (Pincus and Baker 1994). The first and second indirect effects are also termed as the "cloud albedo" and "cloud lifetime" effects, respectively.
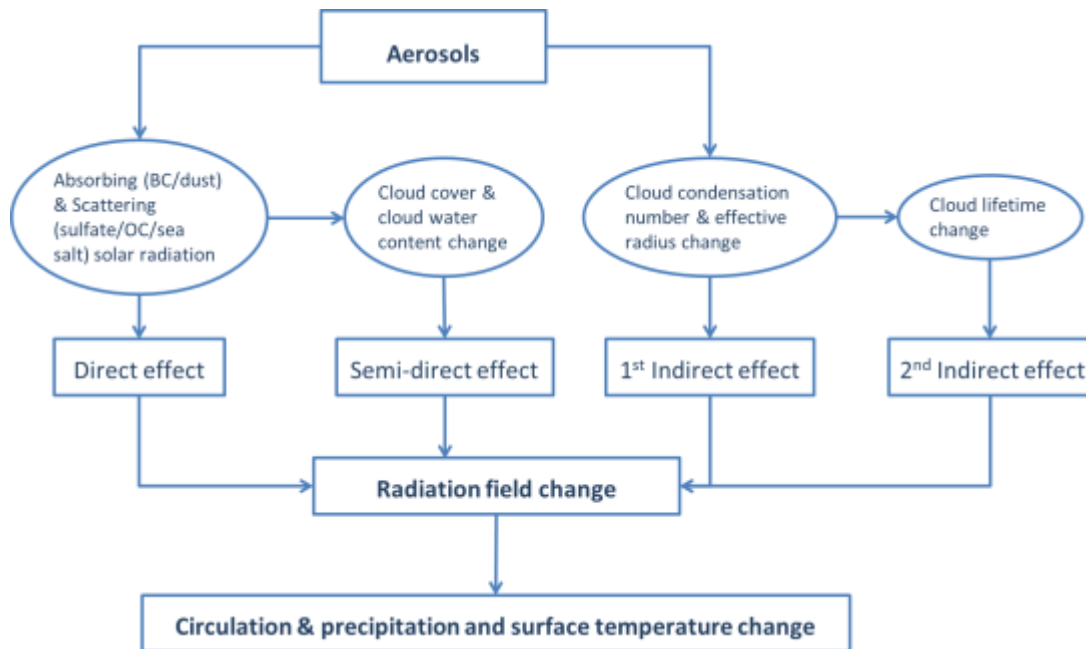


Figure.1 Schematic diagram of the effect of aerosols

This multifaceted influence makes the aerosol one of the least predictable elements in weather and climate modeling (IPCC AR5, 2013). In the past few years, the variety of observations and modelling experiments results in a spread range of aerosol effects on radiative forcing, temperature, precipitations, accompanied by larger differences between observations and model results, and between different models. Take radiative forcing for example, the direct radiative forcing (RF), is given a best estimate of $-0.35$W m$^{-2}$ ($-0.85$ to $+0.15$W m$^{-2}$) in IPCC AR5. For the indirect effect, the estimated range of radiative forcing is even larger. Myhre et al. (2013) in the work of IPCC AR5 suggested a value of -0.45 for aerosol indirect effective radiative forcing[1] (ERF), but the range is estimated to be 0 to -1.2W m$^{-2}$. Besides, the confidence level for the aerosol-cloud interaction was classified as low by IPCC AR5 (2013). By now, several works have been done in order to explain why contradict results exist for the same region and how aerosols influence the regional climate (Xu 2001, Menon et al. 2002, Gu et al. 2006), especially precipitation, through different mechanisms for different regions.

Thus, the aim of this work is to understand and quantify the impact of aerosols on global climate by incorporating a latest aerosol dataset to a general circulation model (GCM). Our first aim is to thoroughly study aerosol indirect effect on ice clouds by incorporating a latest ice-cloud parameterization into the GCM since most former studies focus on offline test. Moreover, former experiments mainly focused on one aspect of aerosol indirect effect, either on ice clouds or on liquid clouds. In comparison, our work attempts to draw a conclusion on the relative importance between both, with further comparison between aerosol direct and indirect effects. This helps to

---

[1] ERF is the change in net TOA downward radiative flux after allowing for atmospheric temperatures, water vapor and clouds to adjust, but with surface temperature or a portion of surface conditions unchanged.

understand the mechanism of different aerosol effects in major monsoon regions and aerosols impact on microphysical processes. This thesis consists of three chapters:

In Chapter 2, we test the direct radiative forcing of aerosols and present the results of interactions between aerosol sand global major monsoon systems. Using a GCM which quantifies the global radiative forcing of aerosol-radiation effect and their spatial distributions, we provide a possible mechanism through which aerosols, especially absorption aerosols, impact the summer rainfall in West Africa, East and South Asia monsoon regions.

In Chapter 3, we seek to probe the impact of aerosol on ice clouds effective radius by applying an advanced ice cloud parameterization in the GCM. Aerosol indirect effect on ice clouds has always been a hard topic because of its inherent complexity. New data from NASA's A-Train constellation (L'Ecuyer and Jiang 2010) coupled with recent developments in climate modeling provides an unprecedented opportunity to review this aerosol-cloud interaction. This work employs one of the latest ice cloud parameterizations developed by Jiang et al. (2011), which correlates ice cloud effective radius (Re_ice) with convective strength and aerosol optical depth to advance the understanding of aerosol indirect effect on cloud and radiation fields. We find that increased aerosol loading reduces ice crystal mean effective size due to aerosol first indirect effect, and further results in less net solar flux and outgoing longwave on top of atmosphere (TOA). TOA net radiation change is largely dependent on relative magnitude of shortwave and longwave change and precipitation changes primarily respond to cooling/warming of atmosphere.

In Chapter 4, we discuss the current work of incorporating a widely used liquid-cloud parameterization (Boucher and Lohmann 1995) to the GCM to study the aerosol indirect effect on liquid clouds. This liquid-cloud parameterization empirically relates cloud droplets number concentration (CDNC) to the sulfate aerosol mass ($mSO4^{2-}$). Monthly mean values of $mSO4^{2-}$ in

4

1850 from AMIP CAM5 have been used for preindustrial experiment (Qian et al. 2015), while climatology monthly mean values of $mSO_4^{2-}$ from GOCART have been used for present-day experiment. We find radiative cooling occurs globally because of the increased cloud albedo resulting from decreased liquid cloud droplets size. Moreover, most radiative cooling occurs in North Hemisphere, where anthropogenic sulfate aerosols locate, such as East Asia and North America.

# Chapter 2

## 2. Aerosol direct effect on global climate variability

### 2.1 Overview of aerosol direct effect

Aerosols, both natural and anthropogenic, could impact energy and water cycles, first through perturbing the radiative components of the energy cycle, and then through feedback processes associated with both the energy and water cycles (Li et al. 2016). The study of aerosol effects starts from the aerosols-radiation interactions to the interactions between aerosol and monsoon system. Due to the development of Earth observing system and global climate models, aerosol effects are better observed, modelled, and understood than ever before.

Aerosol optical depth (AOD, also called aerosol optical thickness), is often used to show the degree to which aerosols prevent the transmission of light by absorption or scattering of light. It is defined as the integrated extinction coefficient over a vertical column of unit cross section (Eq. 1).

$$AOD = \int_0^1 \alpha(z)dz \quad (1)$$

Where $z$ is the thickness of the atmosphere through which the light travels and $\alpha(z)$ is the attenuation coefficient of a specific type of aerosol at level $z$. The attenuation coefficient is mainly determined by various optical properties of aerosols, which include: the extinction coefficient that determines the degree of interaction of radiation and the aerosol particles; the single scattering albedo that determines the degree of absorption; and the symmetry factor that determines the angular distribution of scattered radiation (Kiehl and Briegleb 1993). These parameters are determined as a function of wavelength by assuming spherical particles and by applying Mie

scattering theory to a size distribution of aerosols with a specified refractive index (Haywood and Boucher 2000).

Figure. 2 shows the time average aerosol optical depth (AOD) in 2016 from MERRA-2 Model (https://giovanni.sci.gsfc.nasa.gov/giovanni/). It can be found that most monsoon region, West African Monsoon (WAM), South Asian Monsoon (SAM) and East Asian Monsoon (EAM), are clearly aerosol hotspots, linking aerosol distributions geographically to major monsoon regions. The all-year round aerosol hotspots over the East and South Asian monsoon regions coincides with the industrial mega-city complex of China and India—the major source of anthropogenic aerosols. In this work, we will focus on two major aerosol direct effects, aerosol- radiation interactions and aerosol-monsoon interactions.
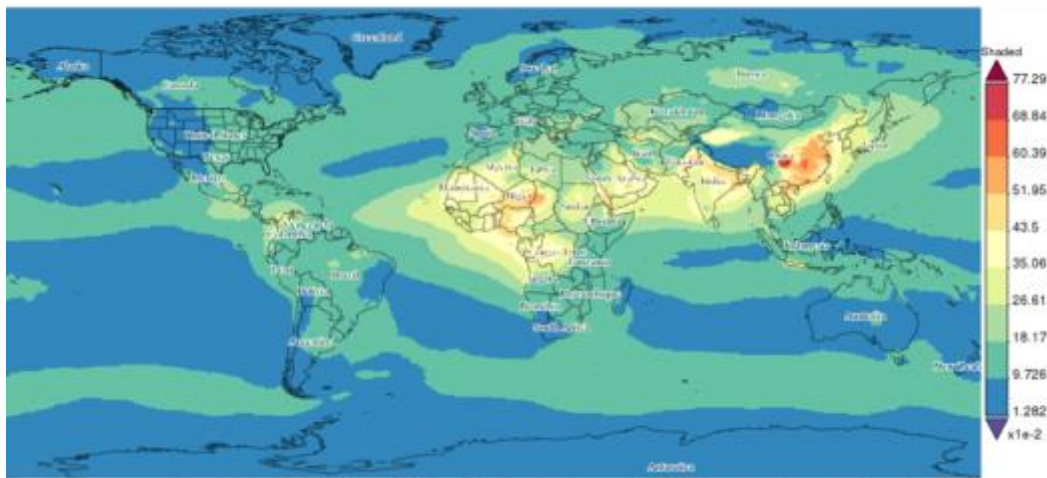


Figure. 2 Time Averaged Map of Total Aerosol Scattering AOT 550 nm monthly
0.5 *0.625 deg. (MERRA-2 Model M2TMNXAER v5.12.4)

### 2.1.1 Aerosol-radiation interactions

Anthropogenic greenhouse gases (GHGs) increases have substantially enhanced the greenhouse effect, and the resulting forcing continues to increase. Aerosols partially offset the forcing of the GHGs and dominate the uncertainty (2013). There are a variety of ways to examine

how aerosols contribute to global climate variability. In principle, observations can directly show the trend of changes in different meteorology components but it's hard to find measurements that are influenced by only a single cause. Climate model is another common way used to study the impact of any single factor. It provides a comprehensive picture of global climate variability and is most commonly used to examine the cause and effect of each forcing. In this study, we mostly focus on analyzing the model results of aerosols.

Global mean calculations of the direct radiative forcing are made up of a series of local column calculations carried out either within a general circulation model (GCM) framework or off-line. Even though more aerosol processes have been included in models, differences between models and observations persist, which may result in larger uncertainties in the aerosol forcing. Despite the large uncertainty range, there is a high confidence that aerosols have offset a substantial portion of global mean forcing GHGs (IPCC, 2013).

The global annual mean radiative forcing of a particular aerosol is determined by its temporal and spatial distribution together with its optical properties. The atmospheric burden is determined by emission processes, chemical reactions, and deposition and transport processes, each of which must be accurately modeled by global chemical transport models (Langner and Rodhe 1991, Penner et al. 1998). The optical properties of aerosols can also depend upon the 3-D geographical distribution of the aerosols. Zhang et al. (2013) attempted to quantify the sensitivities of radiative forcing to dust vertical profiles, especially the discrepancies between using realistic and climatological exponential vertical profiles. They found the use of realistic vertical profile of dust extinction, would lead to greater and more spatially heterogeneous changes in the estimated radiative forcing and heating rate compared to the prescribed vertical profile (Zhang et al. 2013).

Therefore, it is of great importance to apply high-resolution aerosol data retrieved from satellite observations since the aerosol radiative forcing is sensitive to aerosol distribution.

### 2.1.2 Aerosol-monsoon interactions

The monsoon system is one of the most dramatic and important climatic phenomena on Earth, with active energy and water. There has been a rapidly growing body of studies working on the causative factors of the spatial-temporal variability of monsoon system. In the past few decades, surface conditions changes (land cover changes or urbanization) and atmospheric composition changes (e.g., GHGs and aerosols) have been found to alter the monsoon climate (Ramanathan and Feng 2009, Xue et al. 2010).

Many observational data analyses as well as modeling studies has been conducted to understand the role of aerosols on monsoon precipitations. Using a latest GCM, NCEP/GCM/SSiB2, coupled with a three-dimensional aerosol dataset, GOCART, Gu et al. (2015) found that over WAM dust region where dust particles are mainly located to the north of rainfall band, the heating of the air column by dust particles forces a stronger ascent motion over dust layers, inducing an anomalous subsidence and suppressing cyclonic circulation to its south. Precipitations are decreased over WAM region consequently. From GCM experiment, Lau et al. (2006) found that the SAM may be strengthened resulting from atmospheric heating over the southern and northern slopes of the Tibetan Plateau (TP) by the absorption aerosols (dust and BC), through an "elevated heat pump" mechanism. As the warm air rises, the upper troposphere warm anomaly draws in warm moist air from below, leading to forced ascent, enhanced convection, and increased summer monsoon rainfall over northern India.

The aerosol-monsoon interactions over EAM are more complicated. Adding aerosol data to the Goddard Institute for Space Studies (GISS) climate model, Menon et al. (2002) found one of the absorption aerosols, soot may have affected large-scale circulation and the precipitation trends in China over the past several decades, with increased rainfall in the south and decreased rainfall in the north part of China (Menon et al. 2002). However, the prescribed single-scattering albedo (0.85) in Menon's experiment is not consistent with the observed value in China, which is about 0.9 (Lee et al. 2007). Thus, the absorption effect of BC may be exaggerated in Menon et al. (2002). Using an updated version of UCLA AGCM which incorporates a state-of-the-art aerosol/cloud radiation scheme, Gu et al. (2006) investigated the effects of various types of aerosols on radiation budget, temperature, and precipitation patterns in EAM. Their results suggest that different types of aerosol would impact the energy balance in different ways: while scattering aerosols such as sulfate primarily influence incoming solar radiation, absorption aerosols like BC could affect both solar and IR radiation through their absorption and the semi-direct effect on cloud fields (Gu et al. 2006).

These studies have suggested the two-fold effects of absorption aerosols: a heating of the atmosphere that could lead to enhanced precipitation, and a cooling of the surface that may reduce precipitation. Which effect plays a dominant role may depend on model performance and simulated large scale circulation patterns. Furthermore, a recent study on East Asian summer monsoon suggests the location of aerosols with respect to the major rainfall band may also decide whether precipitation is increased or reduced over the monsoon region (Wu et al. 2013). In our study, we will use a global climate model to quantify the global radiative forcing of aerosol-radiation effect and to providing a possible mechanism through which aerosols impact the global major monsoon regions.

## 2.2 Model, datasets and experiment design

### 2.2.1 Model Description and Datasets

The National Centers for Environmental Prediction (NCEP) Global Forecast System (GFS) is modified to simulate the role of aerosols in affecting radiation field and cloud properties. The horizontal resolution of the model is set at T126, which represents 384 longitudes equally spaced and 190 latitudes unequally spaced grid points, approximately $1° \times 1°$ at the equator. 64 vertical levels are used, most of which are in the troposphere. NCEP-GFS is coupled with the second generation of Simplified Simple Biosphere Model (SSiB2) as the land surface model (Xue et al. 1991, Zhan et al. 2003, Xue et al. 2004). In next section, we briefly summarize some parts of the atmospheric model that are most relevant to aerosol effects.

The GFS uses shortwave (SW) radiation parameterization following the NASA approach (Chou et al. 1998; Hou et al. 1996, 2002) and the longwave (LW) radiation parameterization following the GFDL scheme (Fels and Schwarzkopf 1975, Schwarzkopf and Fels 1991). The fractional cloud cover used in the radiation calculation is diagnostically determined by the predicted cloud condensate based on the approach of Xu and Randall (1996). The cloud microphysical processes except auto-conversion are parameterized following Zhao and Carr (1997). This prognostic cloud parameterization scheme includes both cloud water and cloud ice, as well as some microphysical processes for both the convective and grid-scale precipitation production. The auto-conversion parameterization in GFS is based on Sundqvist et al. (1989).

The simulated global aerosol data used in this study are from the GOCART model (Goddard Chemistry Aerosol Radiation and Transport) driven with assimilated meteorology fields from the Data Assimilation System (GEOS DAS) (Chin et al. 2002). The GOCART simulates major tropospheric aerosol components, including sulfate, dust, black carbon (BC), organic carbon

(OC), and sea-salt aerosols, among which dust aerosol has been divided into 5 bin sizes (0.1–1, 1–1.8, 1.8–3.0, 3.0–6.0, and 6.0–10 μm). Three-dimensional monthly averages of the aerosol mixing ratio are available with a horizontal resolution of 1° latitude × 1.25° longitude degrees and 72 vertical layers. The GOCART data also provides the optical properties (i.e., the extinction, scattering and absorption coefficient, single-scattering albedo, asymmetry factor and phase function) of all these five types of aerosols under 36 relative humidity conditions. Single-scattering properties for the various dust size bins are calculated by Mie[2] scattering based on the optical property database in the Global Aerosol Data Set (Koepke et al. 1997).

### 2.2.2 Experiment design

We excluded the slow SST response to aerosol forcing and the feedbacks to the climate system through the air-sea coupling in this study since our first step is to better understand the mechanisms of aerosol direct effects on surface. This methodology has been widely used in previous aerosol-climate interaction studies [e.g., Menon et al. (2002), Lau and Kim (2006), Jiang et al. (2013)]. In this work, we conducted model simulations from January 1, 2006 to December 31, 2011 using a prescribed climatology SST from WAMME II (Xue et al. 2016) to exclude the feedback from the global ocean. The first year has been used for initialization and the last five years have been made averaged for analyses, and we focus our attention on results for June – July – August (JJA). Our experiment design is listed as below:

CTL: in the control case (CTL), the aerosol effects are excluded from model simulations by turning off aerosol data for either direct or indirect effects.

---

[2] **Mie scattering:** In atmospheric science, Mie scattering occurs when the diameters of atmospheric particles are similar to the wavelengths of the scattered light. <u>Dust</u>, <u>pollen</u>, <u>smoke</u> and microscopic water droplets are common causes of Mie scattering. Mie scattering occurs mostly in the lower portions of the atmosphere where larger particles are more abundant, and dominates in cloudy conditions.

DIR: in the DIR case, only the aerosol direct radiative effect is accounted for by incorporating the GOCART data.

The differences between DIR and CTL are used to assess the climatic effects of aerosols due to its direct/semi-direct radiative forcing.

## 2.3 Aerosol experiments and Results

Figure 2.1 illustrates the global JJA mean total AOD from 1998 to 2010 from GOCART dataset. Total AOD have the largest magnitude over North Africa and Asia during June–July–August (JJA), among which the major dust belt extends from North Africa to Middle East, Central and South Asia as well as across the Atlantic to the southeast United States. Most sulfate aerosol distributes in north hemisphere, mainly in East Asia and North America (Not shown). The BC distribution is similar to that of sulfate, except for tropical forest regions where biomass burnings release a large portion of soot.
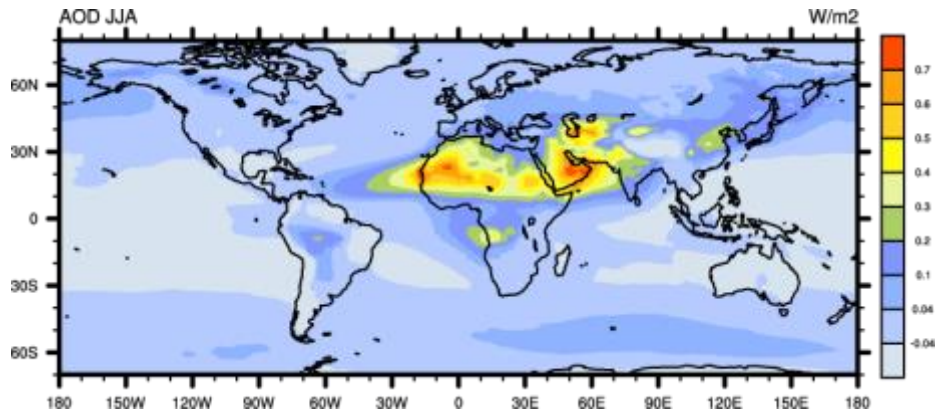


Figure 2.1. 1998-2010 JJA climatology AOD distribution in GOCART dataset

Figure 2.2a displays the surface downward shortwave (SDW) difference between DIR and CTL. The cross represents differences that are statistically significant at a significance level of 0.1.

Figure 2.2a shows that SDW has decreased due to absorption and scattering by aerosols in the atmosphere. The areas with main aerosol impacts cover two major monsoon system regions in summer: North Africa and tropical north Atlantic region and the South/East Asia region. We mainly focus on these regions for further analysis.

The larger net radiation on TOA over North Africa, Middle East, and South Asia results from the absorbing effect of absorption aerosols such as dust and black carbon. This mainly occurs on land area because absorption aerosols have relative smaller albedo than the land surface while larger albedo than the ocean (Figure 2.2b). East Asia is affected by both dust and sulfate aerosols and the total effect are shown to be slightly negative (Figure 2.2b). The net radiative forcing on surface can be as large as -30 W·m$^{-2}$ (Figure 2.2c), primarily results from shortwave forcing and is also adjusted by longwave forcing (not shown).
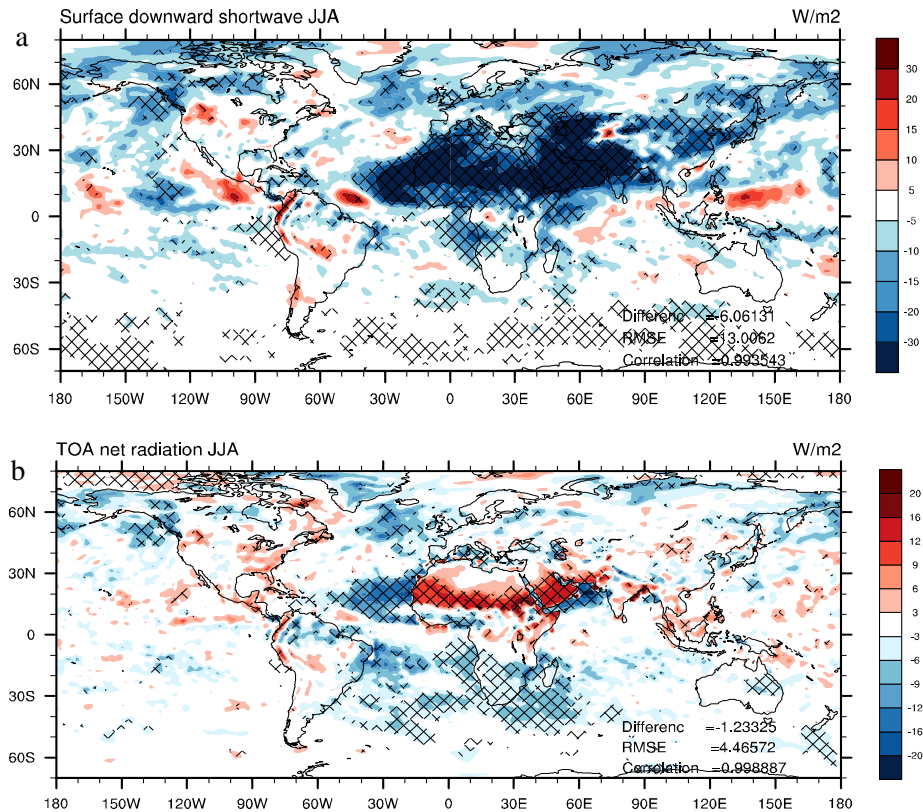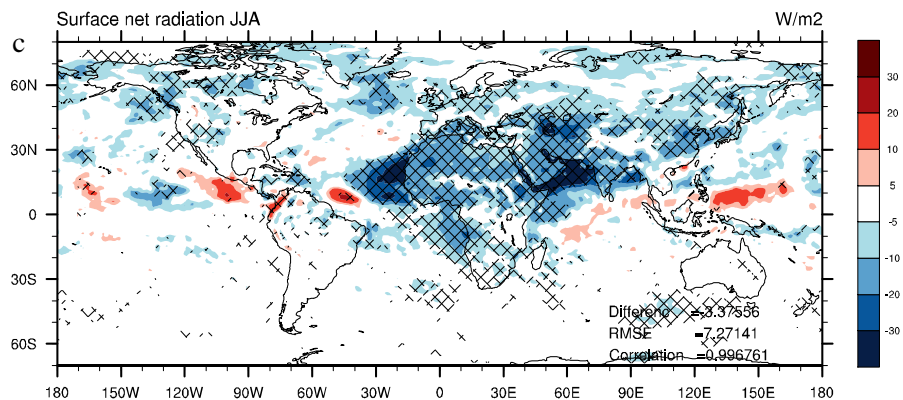
Fig 2.2 Difference of a) Surface DSW b) TOA net radiation c) Surface net radiation between DIR and CTL in JJA

Figure 2.3 shows the JJA mean differences of precipitation between DIR and CTL. Due to aerosol effect, especially absorption aerosols (dust and BC), precipitation is increased over West Africa, the coastal region of West Africa, and Northwest India (Figure 2.3a). Meanwhile, precipitation reduction can be found over Central Atlantic, North Indian Oceans by compensation. In fact, absorption aerosols change the large-scale circulation by heating the low-to-middle-level air, increasing the upper motion over the aerosol region and bringing more moisture inland. Consequently, these in turn could favor an increase in continental precipitations through an enhancement of monsoon systems. Figure 2.3b shows the effect of aerosols on cloud cover. The cloud cover change is a good indicator for convection change. In South Asia where cloud cover is found to increase due to strengthened convection, precipitation also increases. The main surface temperature decreases can be found in land area in North Hemisphere (Figure 2.3c), in response to radiation change, especially for regions where most aerosols are located, WAM, SA and Northern China. Note that the SST forcing is fixed in this study so there is no change of surface temperature over the ocean.
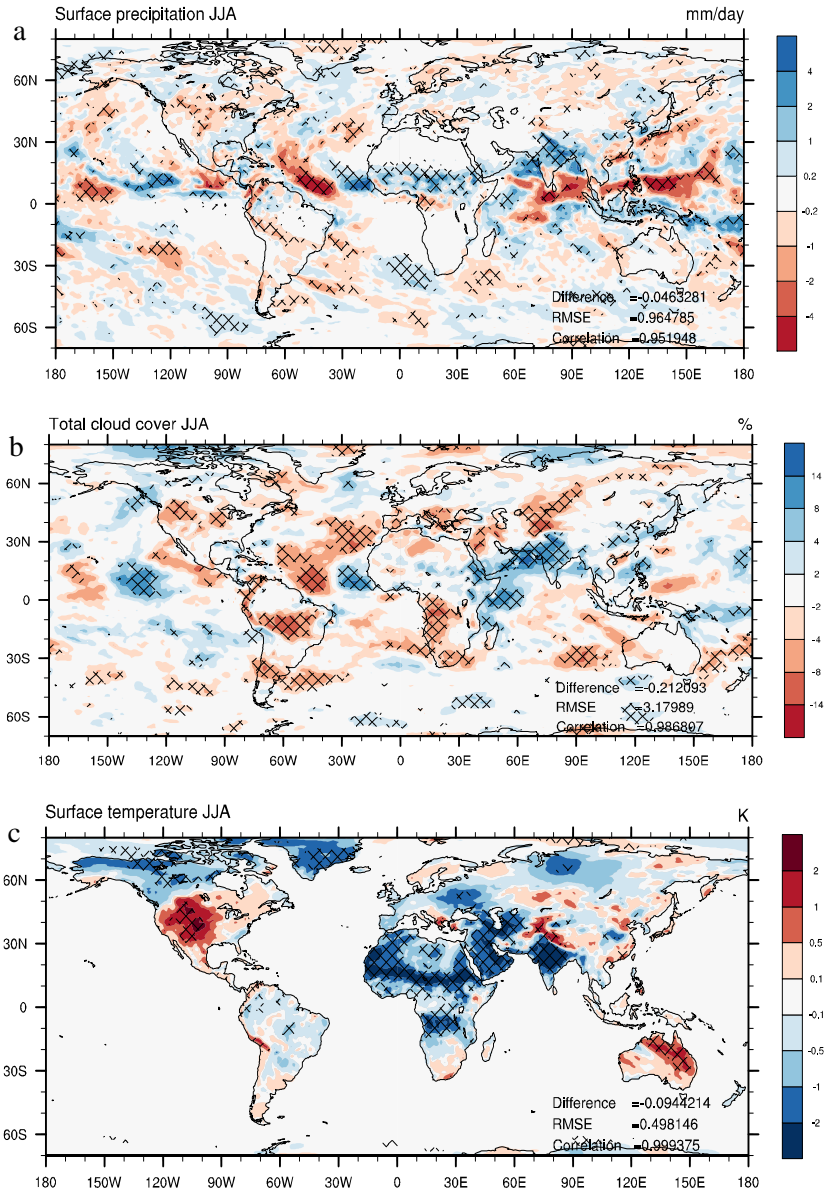
Figure 2.3. JJA mean difference in a) Precipitation b) Cloud Cover c) Surface Temperature between DIR and CTL.

To better understand the mechanism which causes precipitation changes, we use West Africa monsoon regions as an example to further analyze the role of aerosols on regional circulation (Figure 2.4a). In the North Africa, where the dust heating prevails, the positive vorticity

and the cyclonic circulation are produced (Figure 2.4b). The ascending motion in North Africa results in stronger moisture flux and vertically integrated moisture flux convergence in Sahel region, thus enhancing the precipitation in West Africa (Figure 2.4a).
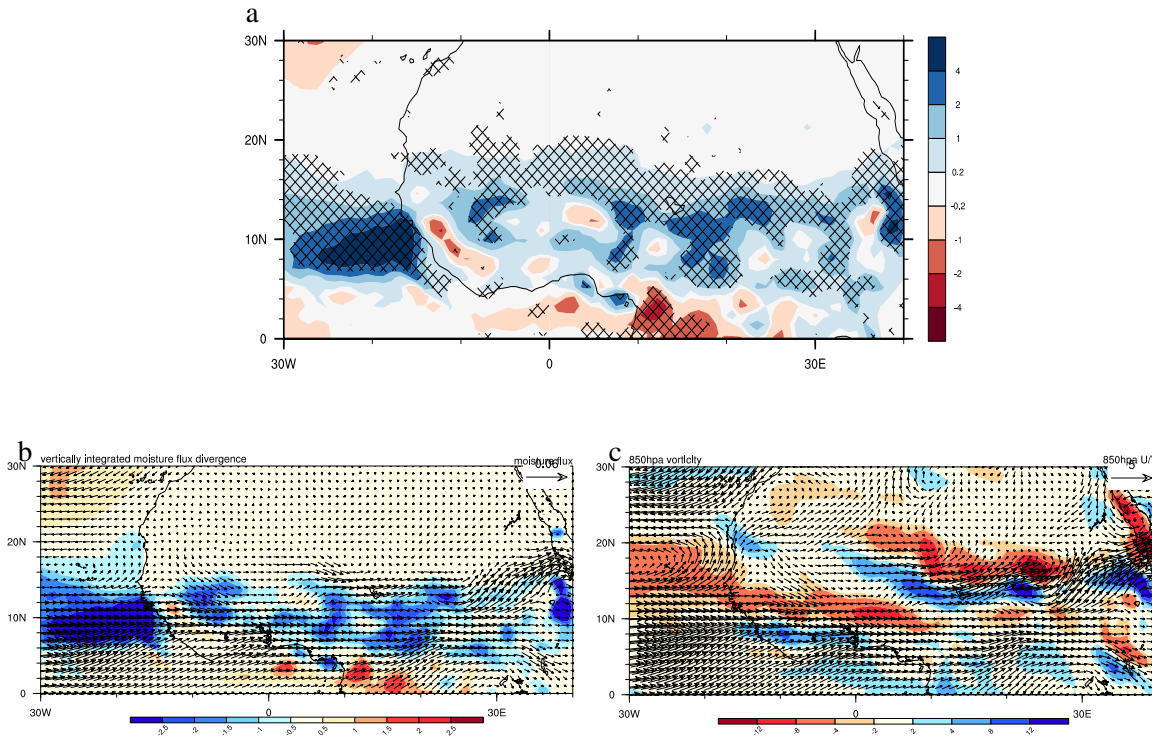


Figure 2.4. Mean differences in a) Precipitations b) Moisture Flux (vector, m/s) at 850 hPa and vertically integrated moisture divergence (shaded, mm/day), and c) 850hPa wind (vector, m/s) and vorticity (shaded, $10^{-6}$ s$^{-1}$) between Case1_DIR and Case1_CTL for West Africa in JJA

A similar conclusion can be drawn from the pressure/height streamline and temperature at 5°E in JJA (Figure 2.5). Due to higher temperature over the land surface, the monsoon inflow can be found near 5°N and extends to 15°N, and is confined below 850hPa, with ascending motion across these latitudes. These regions correspond to the area with largest precipitation. The upward motion below 600 hPa around 15°N–25°N is constrained by the anticyclonic circulation of the Saharan high, which produces subsidence in the upper troposphere (200 –600 hPa) and acts as the

north barrier of the WAM. Figure 2.5b shows the difference of pressure/height streamline and temperature, from which we can see absorption aerosols (dust and BC) over the Sahara at 20°N–30°N heat the low-to-mid-level air, resulting in increased upper motion and enhanced convection in 15°N–25°N in middle layer. This upward motion brings about descending motion at around 5°N, which produces cyclonic circulation in middle layer. This cyclonic circulation further brings about upward motion in the same latitude in the lower level, which resulting in increased precipitation over West Africa. Our conclusion is consistent with the "elevated heat pump" mechanism proposed by (Lau et al. 2009).
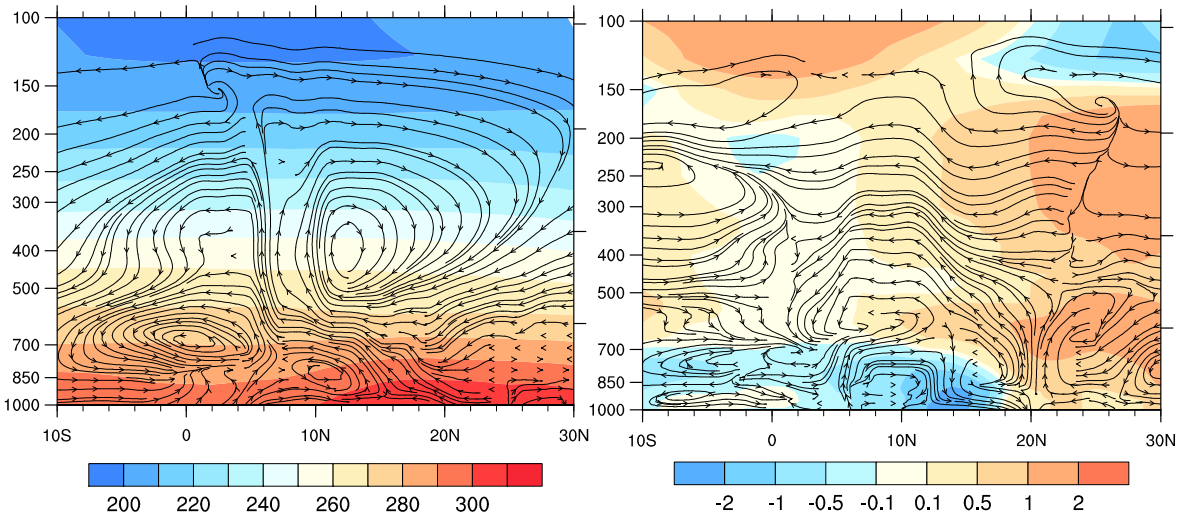


Figure 2.5 Latitude-height cross section of a) Streamline (v; −ω × 100) and Temperature (K, *shaded*), and b) their differences between DIR and CTL at 5°E in JJA

Precipitation change in South Asia is also caused by "elevated heat pump" mechanism with regional topographic difference. In East Asia, interactions between aerosol and monsoon is more complex because both dust and sulfate aerosols play an important part. Scattering aerosols such as sulfate affect precipitation through different mechanism, which will not be discussed in this thesis.

# Chapter 3

## 3. Aerosol indirect effect on ice clouds and global climate variability

### 3.1 Overview of aerosol indirect effect on ice cloud

The previous study of aerosol-radiation and aerosol-monsoon interactions provides a much better understanding of the aerosol direct effect. It has been widely acknowledged that aerosols also influence global climate through their indirect effect. Thus, in *IPCC AR5* (2013), aerosol-cloud interaction (ACI) has been defined as any associated change initiated by changes in cloud microphysics by cloud condensation nuclei (CCN) or ice nuclei (IN).

This influence of aerosol particles on cloud field has been observed and tested in laboratory since 1970s and a lot of progress has been made (Twomey 1974, Hegg et al. 1993, Brenguier et al. 2000, Feingold et al. 2003). For ice clouds, various heterogeneous ice crystal nucleation modes have been found in laboratory studies as well as field observations (Diehl and Mitra 1998, Karcher and Lohmann 2003, Kärcher et al. 2006). Aerosols can act as ice nuclei (IN) by coming into contact with super-cooled cloud droplets (contact freezing) (Kärcher and Lohmann 2002), or by initiating freezing from within a cloud droplet by immersion or condensation freezing (Hoose et al. 2010), or by acting as deposition nuclei (DeMott et al. 2003). Different ice nucleation processes lead to changes in cloud droplets concentration number (CDNC) and cloud particle size, which further affect radiation budget on both TOA and surface.

However, current GCMs rarely include the effect of aerosols in ice cloud parameterization, mainly because of the large uncertainties in ice cloud nucleation modes and limited computational resources (Gu et al. 2012). Some GCMs use prescribed ice particle sizes in consideration of

computational cost (Ho et al. 1998, Gu et al. 2003). Others also build the parameterization by relating ice crystal size to ice water content (IWC[3]) and temperature (Kristjansson et al. 2005). In recent years, new data from NASA's A-Train constellation (L'Ecuyer and Jiang 2010) coupled with recent developments in climate modeling provides an unprecedented opportunity to taking into account the effect aerosols on cloud droplets size in GCMs. Therefore, in this study, we investigate aerosol indirect effect on ice cloud by incorporating the latest ice cloud parameterization developed by Jiang et al. (2011) which expands from traditional Re–IWC relation to Re-IWC-AOD relation into GFS.

## 3.2 Description of a latest ice cloud parameterization

We follow the approach presented by Jiang et al. (2011), in which ice crystal size is related to both aerosol optical depth (AOD) and IWC. This approach assumes the effects of convection and AOD on effective radius (Re) to be independent while actually they are not (Jiang and Su 2010). It excludes the interactions between microphysical and dynamical processes as they are not adequately understood and may contribute to large uncentainties in model simulations. This formulation uses least squares fitting to match A-Train observations and derives an analytical formula to describe the ice cloud effective radius (Re) variations with convection and aerosol optical depth (AOD):

$$Re = \varepsilon \cdot AOD^{\eta} \cdot \left[1 - exp\left(-\frac{CONV_i}{\alpha}\right)\right] \cdot exp(-\beta \cdot CONV) \quad (2)$$

---

[3]**Ice Water Content**: Cloud ice water content (IWC) is defined as cloud ice mass in unit volume of atmospheric air. It can vary largely from 0.0001 g/m3 in thin cirrus to 1 g/m3 inside convective core. The vertically integrated column of IWC is ice water path (IWP)

The equation has three different terms which represent different processes. The first term, $Re = \varepsilon \cdot AOD^{\eta}$ represents the modulation of AOD on Re where $\eta$ is a parameter determining how strong the aerosol effect is, and $\varepsilon$ is a scaling constant. The second term, $[1 - exp(-CONV_i/\alpha)]$, represents the growth of Re with respect to convection. The convective index $(CONV_i)$ is defined as $CONV_i = IWC_i/\overline{IWC}$, where $IWC_i$ represents an individual measurement of 215 hPa. $\overline{IWC}$, is the mean of all 215 hPa measurements (Jiang et al. 2011). The third terms, $1/exp(\beta CONV_i)$, is formulated to model the decrease of Re with $CONV_i$, especially at large $CONV_i$ values. $\varepsilon$, $\alpha$, $\beta$, and $\eta$ are parameters determined by performing a two-dimensional least-squares fitting to the observed data (Jiang et al. 2011). This approach provides an example to seperate dynamic effects from aerosol microphysical effects and at the same time to establish a framework for parameterization of aerosol effects on Re in climate models.

## 3.3 Data and experiment design

Similar experiment design has been adopted in this work as we did to test aerosol direct effects. We ran the model from January 1, 2006 to December 31, 2011 with GOCART climatology dataset from 1998 to 2010 (Chin et al. 2002) and a prescribed climatology SST from WAMME II (Xue et al. 2016). Both control and sensitivity experiments use the latest ice cloud parameterization from Jiang et al. (2011), with different AOD values. Aerosol direct effects are also included in both experiments by employing GOCART data in radiative processes. The experiment design is summarized as follow:

DIR: in the DIR case, the Re-IWC-AOD relationship is used everywhere with a background AOD of 0.01. Aerosol direct radiative effect is accounted for in this experiment. This

experiment is considered as the control run, which represents the case with only aerosol direct effect.

ICE: in the ICE case, both aerosol direct and indirect effect are accounted for by adopting the GOCART data.

The differences between ICE and DIR are used to assess the climatic effects of aerosols due to its indirect effect.

## 3.4 Aerosol experiments and Results

We first evaluate the indirect radiative effect of aerosols by comparing the 5-year simulation results of the experiments ICE and DIR. Figure 3.1 shows ice cloud effective radius (called Re_ice afterwards) difference between ICE and DIR. Decreased Re_ice has been found globally, especially in West Africa, East/South Asia, and in Central Atlantic and is highly related to aerosol loading (Figure 2.2). The maximum change occurs in North Indian Ocean where the magnitude can be more than -3µm.
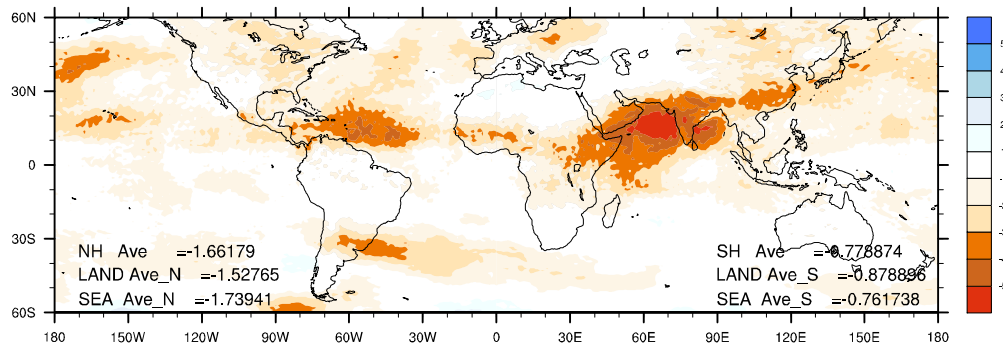


Figure 3.1 Difference of ice cloud effective radius (Re_ice) between ICE and DIR in JJA

The change of cloud droplets size affects radiation budget at TOA according to aerosol first indirect effect (Figure 3.2 a-c). At TOA, net shortwave radiation decreases because ice clouds

22

with smaller sizes reflect more solar radiation. Outgoing longwave radiation also decreases because smaller cloud droplets trap more IR radiation. Both shortwave and longwave changes are affected by both cloud properties and cloud cover. The net radiative forcing is the combination of shortwave and longwave forcing and is closely related to the magnitude of Re_ice change. When Re_ice change is less than $2\mu m$, the change of net solar radiation competes that of longwave radiation. Consequently, the radiative forcing is negative. When Re_ice change is larger than $3\mu m$, the scenario is reversed: the longwave forcing plays a more important role, thus resulting in positive radiative forcing.
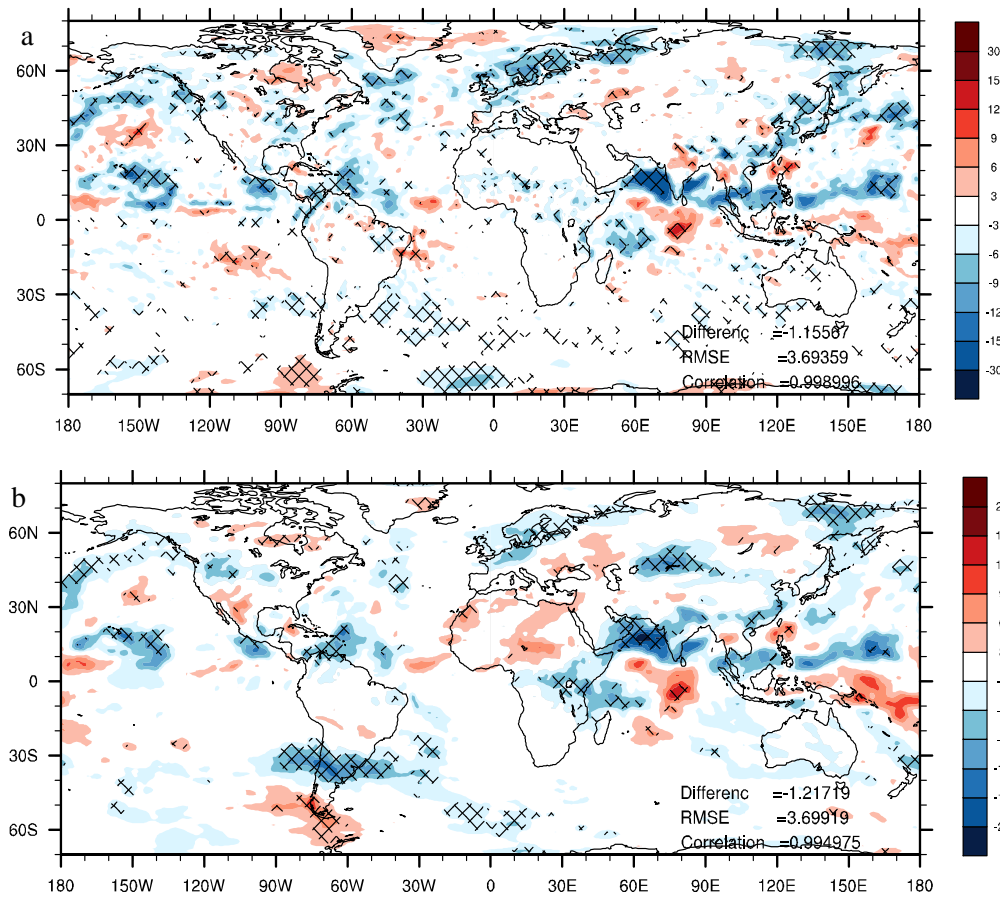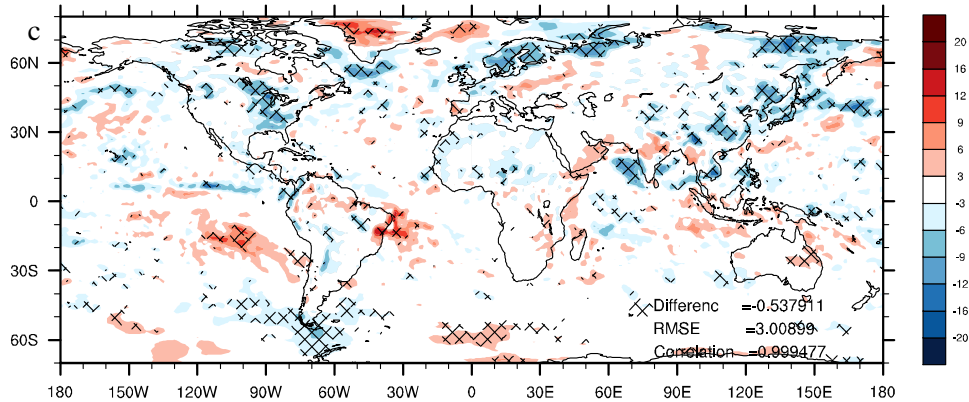
Figure 3.2 Difference of a) TOA net SW (W/m^2) b) TOA ULW (W/m^2) c) TOA net radiation (W/m^2) difference between ICE and DIR in JJA

The change of radiation budget from Re_ice change also affects vertical motion and cloud cover, the latter one affects radiation budget in return. Decreased net radiation in the atmosphere over West Africa, Northern China and East America leads to less ascending motion while increased net radiation over East and North boundary of Indian ocean, Southeast Asia leads to more upper motion at 500hPa (Figure. 3.3a). The change of vertical motion directly affects cloud IWC: when upward motion is suppressed, clouds will contain less ice water (Figure 3.3b), which also happens for liquid water (not shown). The change of ice water content is consistent in different levels from 100mb to 400mb (not shown). Precipitation and cloud cover change show a similar pattern to that of IWC in association with the change in convection strength (Figure 3.3c-d). Here we mainly focus on high cloud cover because ice clouds normally exist at high altitude.
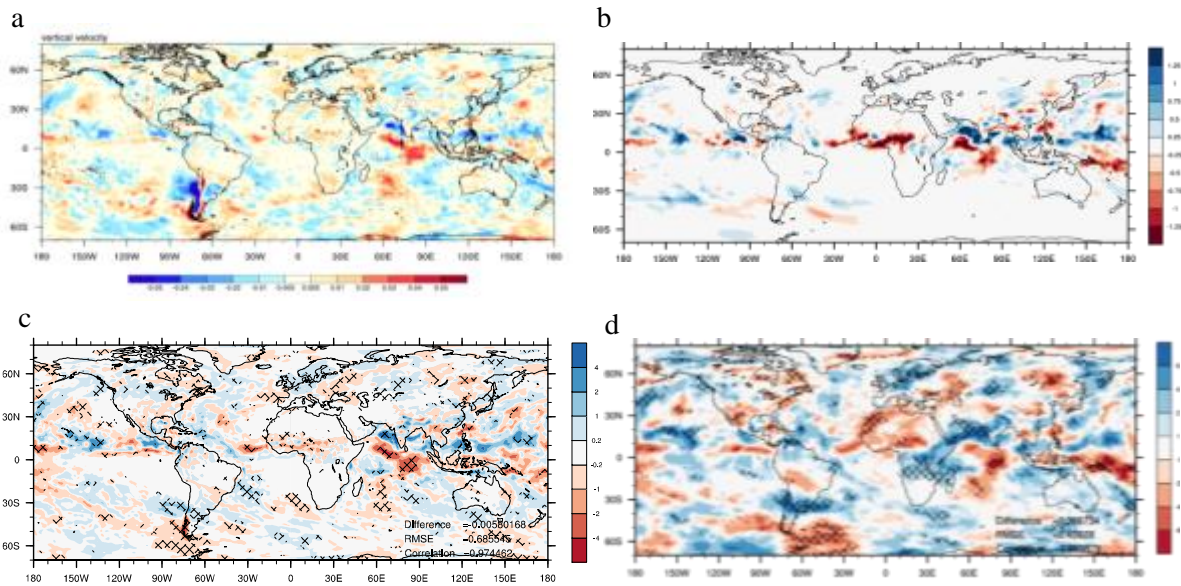
Figure 3.3 Change of a) Vertical velocity (Pa/s) b) 200mb Ice water content (kg/kg) c)

Precipitation (mm/day) and d) Cloud cover (%) between ICE and DIR in JJA

The change of surface net radiation shows some consistency to that of TOA net radiation change (Figure 3.4a). Surface net radiation has been decreased by more than $1W/m^2$ globally. Net radiation on most North Hemisphere land area decreases, resulting from decreased surface radiation budget. However, the increased surface temperature in South Asia (Figure 3.4b) is relating to the increased precipitations, which leads to more evaporation and more latent heat flux at the same time.
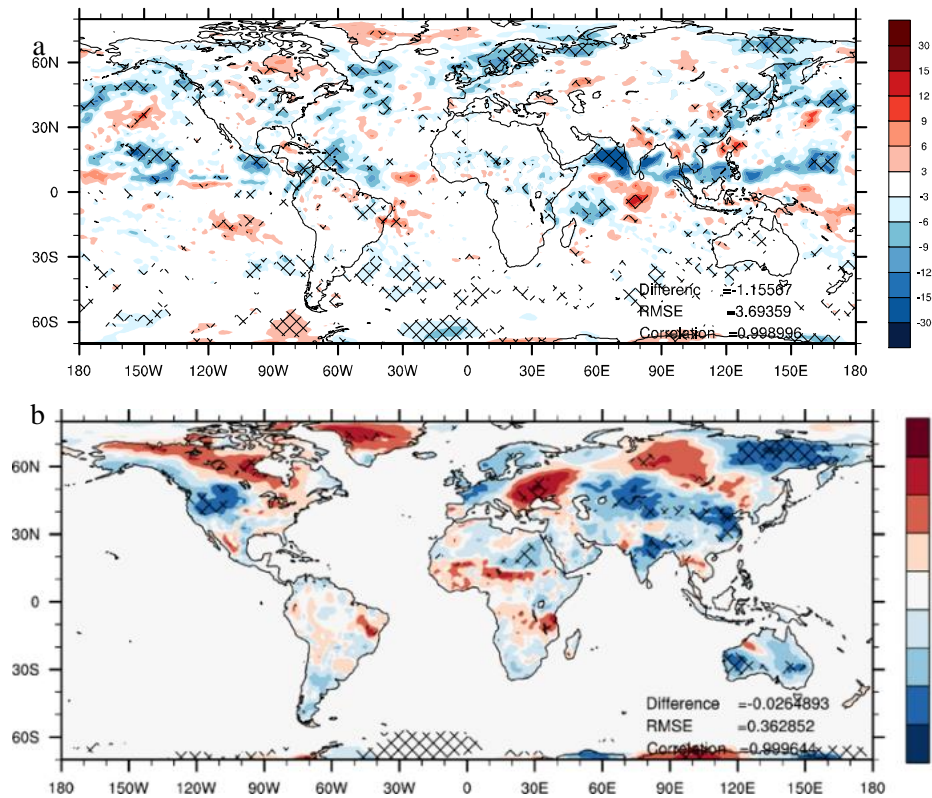
Figure 3.4 Differences of a) Surface net radiation (W/m^2) and b) Surface TMP (K) between ICE
and DIR in JJA

It should be noted that most GCMs, including the GFS, do not consider cloud droplets size

change in their microphysics processes (Gu et al. 2012). So the normally defined aerosol second

indirect effect (e.g., the effects of smaller cloud droplets on auto-conversion rate and cloud life-

time) is not included. The differences in precipitation distribution patterns, therefore, are

associated with the interactions and feedback among aerosols, radiation, clouds, and dynamic

fields which are modulated by the first indirect aerosol radiative forcing and in turn affect the

simulated climate.

# Chapter 4

## 4. Aerosol indirect effect on liquid clouds and global climate variability

### 4.1 Overview of aerosol indirect effect on liquid cloud

Aerosol impacts on warm clouds[4] are relatively less complicated because only the liquid phase is involved. Still, several types of aerosol indirect effects have been proposed (Twomey 1974, Albrecht 1989, Kaufman and Fraser 1997). Former work has systematically showed the present of aerosol can lead to a decrease in cloud effective radius (Re) with an increase in aerosol concentration under fixed liquid water path[5] (LWP) conditions, called first indirect effect (Feingold et al. 2003, Kim et al. 2008). This implies an increase in the albedo of a cloud, resulting in enhanced reflection and a cooling effect (Twomey 1974).

Smaller cloud effective radius also means it takes longer to reach sizes that are large enough to precipitate. This effect, called cloud second indirect effect or cloud lifetime effect, may enhance cloud cover, imposing an additional surface cooling (Albrecht 1989). Drizzle suppression in polluted air has been consistently observed and simulated, mainly due to the mechanism of a less efficient collision/coalescence process resulting from the smaller cloud droplet size (Albrecht 1989). However, cloud lifetime increase is not as significant as precipitation suppression because the increased aerosol concentrations enhances evaporative cooling thus creating a temperature contrast with the surrounding warm air (Li et al. 2016). The enhanced contrast generates an

---

[4]**Warm clouds**: The evolution of clouds that follows the formation of liquid cloud droplets or ice crystals depends on which phase of water occurs. A cloud in which only liquid water occurs (even at temperatures less than 0 °C) is referred to as a warm cloud, and the precipitation that results is said to be due to warm-cloud processes.
[5]**Liquid water path**: in units of [kg/m²] is a measure of the total amount of liquid water present between two points in the atmosphere.

increased vorticity around cloud boundaries, making faster convective turnover and leading to shorter cloud lifetime shorter (Jiang et al. 2006, Lee et al. 2012). This suggests that, in addition to microphysical impact of aerosol effects on cloud droplet size, aerosol-induced changes in thermodynamics and dynamics should be considered for a more comprehensive understanding of ACI.

Attempts to estimate the magnitude of liquid cloud indirect effect has been done by Chuang et al. (1993). A climate model together with a 3-D chemical transport model was used in their experiment and the cloud nucleation parameterization included aerosol number, sulfate mass concentration and updraft velocity. The work of Jones et al. (1994) also related the sulfate aerosol mass to cloud droplets number concentration (CDNC) through empirically-derived relationships. Boucher and Lohmann (1995) applied a different empirically-derived approach to parameterize the sulfate-CDNC relationship. This work presented a detailed comparison with previous estimates and discussions about the remaining uncertainties. This parameterization has been widely used since 1990s.

## 4.2 Description of a widely-used liquid cloud parameterization

In this work, we also employ the empirically-derived parametrization related cloud droplets number concentration (CDNC) to the sulfate aerosol mixing ratio ($mso_4^{2-}$) developed by Boucher and Lohmann (1995), which can be expressed as:

$$CDNC = 10^{2.21+0.41\log(mso_4^{2-})} \quad (2)$$

The next step is to relate CDNC to the droplet effective radius, $R_e$, a key parameter to determine shortwave radiative properties of clouds. $R_e$ is defined as:

$$R_e = \frac{\int r^3 n(r) dr}{\int r^2 n(r) dr} \quad (3)$$

Field measurements suggest a linear regression between cloud effective radius, $R_e$ and volume averaged cloud droplet radius, $R_3$

$$R_e = 1.1 R_3 \quad (4)$$

$R_3$ can be explicitly calculated from CDNC and in-cloud liquid water content[6] (LWC):

$$R_3 = \left( \frac{LWC \rho_{air}}{\left(\frac{4}{3}\right) \pi \rho_{water} CDNC} \right)^{1/3} \quad (5)$$

The combination of Eqs. (2), (3), (4) and (5) eventually relates $R_e$ to CDNC.

This parameterization has generated a lot of similar results among different GCMs (Lohmann and Feichter 1997, Kiehl et al. 2000, Ming et al. 2005). This consistency slightly increases our confidence that some main processes of aerosol-cloud interactions are being captured. However, the rather good agreement among different GCMs is by no means implies a solution to aerosol-cloud interactions. There still exist large uncertainties among GCMs, such as precipitation and cloud cover change pattern, because of different cloud schemes. Moreover, the range of aerosol indirect radiative effects is still too large, about 1.4-4.8 W/m^{2} reported by Lohmann and Feichter (1997). Therefore, more experiments are needed to inspect aerosol effects on various aspects and on different time and spatial scale. In this work, we incorporated the same relationship in GFS (Boucher and Lohmann 1995), but differs from the previous studies in terms of cloud amount, microphysics, and auto-conversion schemes (Lohmann and Roeckner 1996, Rotstayn 1999) . Our work also tests the practicality of using the GFS as a tool for studying aerosol indirect

---

[6]**Liquid water content:** the measure of the mass of the water in a cloud in a specified amount of dry air. It is typically measured per volume of air (g/m3) or mass of air (g/kg)

effects on liquid clouds.

## 4.3. Data and model and experiment design

This work still uses GFS to study aerosol indirect effect as a continuation of former work. We used climatology sulfate mixing ratio in 1998-2010 from GOCART to represent present-day aerosol loading. For pre-industrial case, we made average of 256 model runs from AMIP CAM5 and used the ensemble mean sulfate mixing ratio (Qian et al. 2015). The experiments designs are listed as follow:

Case_PI: Empirically-derived liquid cloud parametrization by Boucher and Lohmann (1995) has been applied, while ensemble mean sulfate mixing ratio from AMIP CAM5 has been adopted to represent pre-industrial aerosol forcing.

Case_PD: The sensitivity experiment applies the same parametrization (Boucher and Lohmann 1995), while sulfate mixing ratio from GOCART has been adopted to represent present-day aerosol forcing.

Comparisons between Case_PD and Case_PI demonstrate climate effect of aerosol indirect effect on liquid clouds.

## 4.4 Aerosol experiments and Results

Figure 4.1a-b show the distribution of sulfate aerosol mixing ratio in pre-industrial and present-day case in the first layer of GFS. Pre-industrial sulfate aerosol loadings mainly come from natural sources, such as forest fire or oxidation of dimethyl sulfide (DMS) emitted from the ocean. Present-day sulfate aerosol mostly located over continents of Northern Hemisphere, with maxima over East and South Asia. Industrial sulfate aerosols are produced by oxidation of $SO_2$ and emitted

from anthropogenic activities such as coal burning (Chin et al. 2002). Its relatively short lifetime

makes its spatially heterogeneous distribution: the source regions (East Asia, South Asia, Europe

and East America) normally have larger aerosol concentrations. The change of liquid cloud

effective radius (Re_liquid) is a direct reflection of increased sulfate aerosol mass concentration

(Figure 4.2a). The latitudinal averaged Re_liquid change varies with latitude in both North and

South Hemisphere, with its largest changes in mid-latitude (Figure 4.2b).
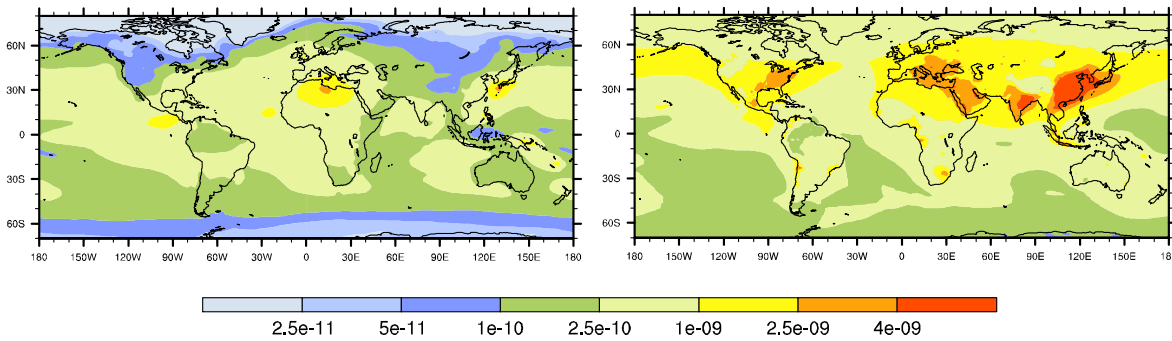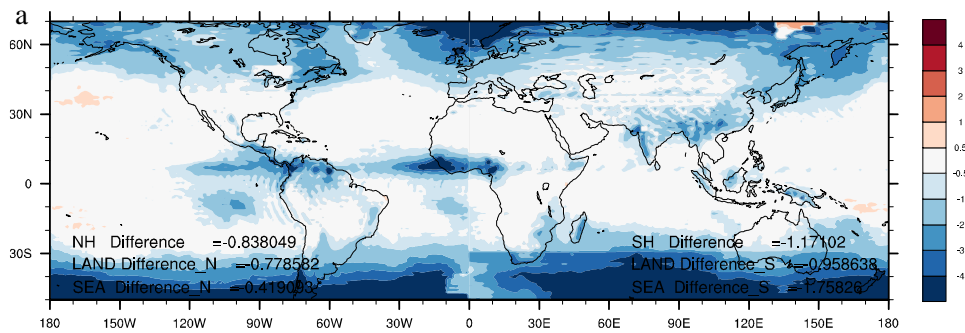


Figure 4.1 First layer sulfate aerosol mixing ratio in present day (Case_PD) and pre-industrial
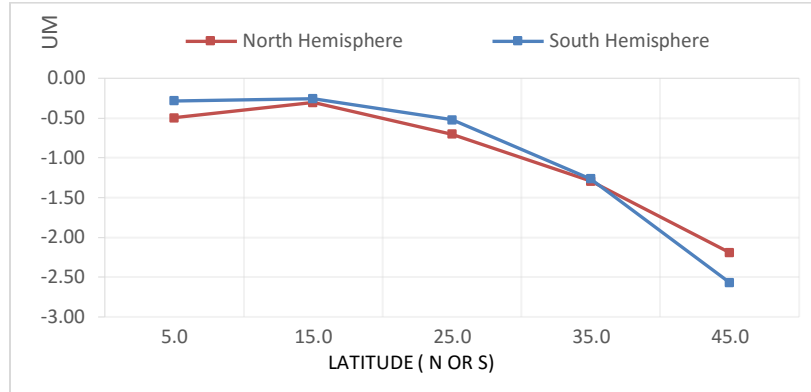
(Case_PI) experiment (kg/kg)

Figure 4.2a) Simulated distribution of difference of liquid cloud effective radius (um) b) latitudinal averaged difference in liquid cloud effective radii (um) on 850 hPa in JJA

Liquid clouds with smaller droplets size have larger albedo and are able to reflect more solar radiation, thus increasing global upward shortwave radiation, especially over North Hemisphere continent where most Re_liquid changes occur (Figure 4.3a). The longwave radiative properties of liquid clouds and the liquid-phase of mixed cloud has been neglected according to Boucher and Lohmann (1995), because most of them are thick enough to act as black bodies. Longwave radiation changes primarily according to cloud cover change (not shown). The geographical distribution of net radiation change on TOA is similar to shortwave change since the longwave adjustment plays a small part. Very few regions show a positive flux changes, most of which are located at the ocean. Surface net radiation also reduce in response to increased cloud albedo (Figure 4.3c), which leads to decreased surface temperature (Figure 4.3d). Increased temperature can be found over West Africa despite of the decreased net radiation, which results from increased regional precipitation (Figure 4.4b) and evaporation, indicating the precipitations

change the energy partitioning between sensible heat, latent heat and ground heat flux, which further adjust the surface temperature.
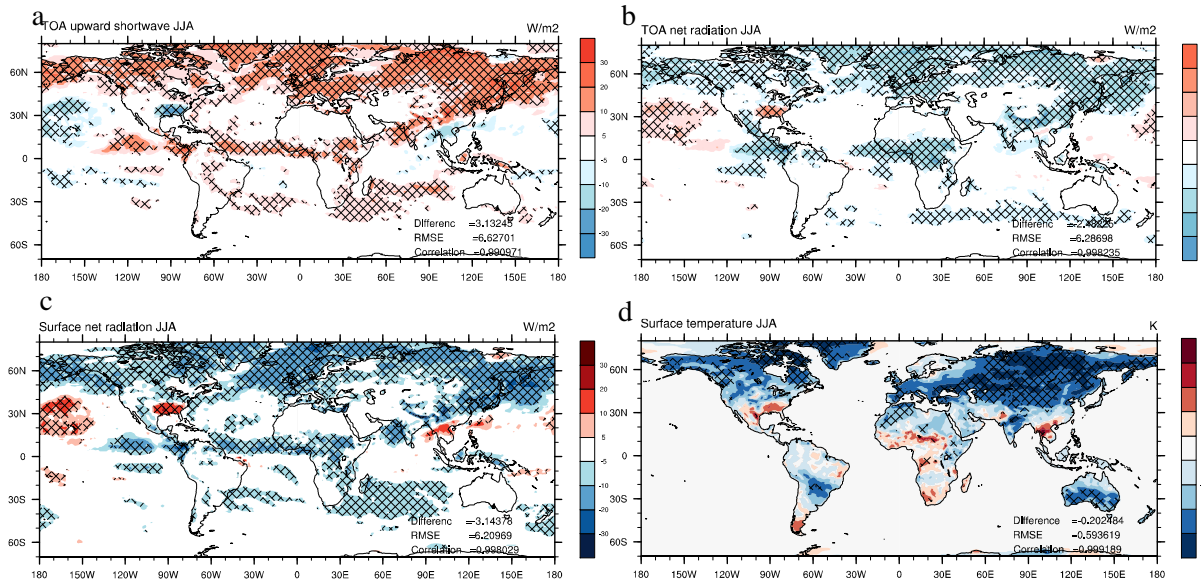


Figure 4.3 Difference of a) TOA upward shortwave (W/m^2) b) TOA net radiation(W/m^2) c) Surface downward radiation (W/^2) and d) Surface TMP (K) between Case_PD and Case_PI in JJA

The decreased net radiation results in descending motion over land (Figure 4.4a). Suppressed vertical motion and decreased radiative forcing reduce the land-sea air temperature contrast over West Africa and East Asia and thus disturbing the monsoon system (Figure 4.5). Moisture flux divergence can be found at 850hPa over West Asia and East Asia monsoon systems, which reduces inland water vapor transport from the ocean. The precipitation decreases in response to decreased moisture flux over land.
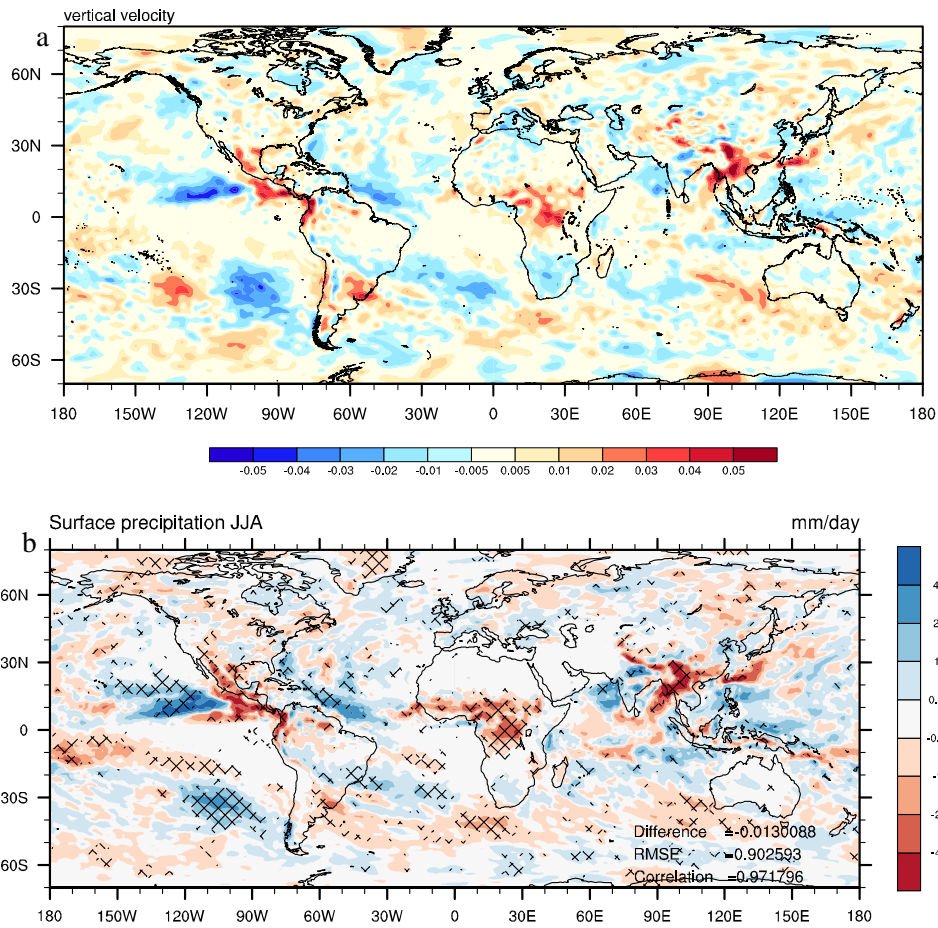
Figure 4.4 Differences of a) Vertical velocity at 500hPa (Pa/s) b) Precipitation (mm/day) between
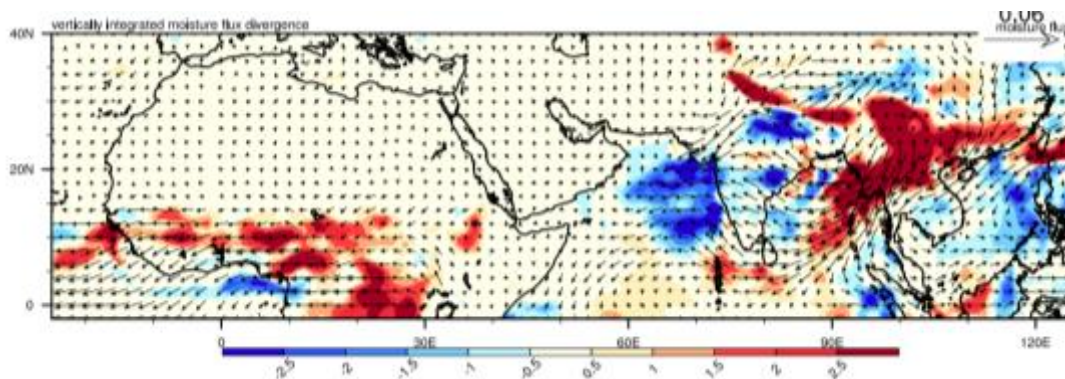
Case_PD and Case_PI in JJA



Figure 4.5 Difference of 850hPa moisture flux (vector) and vertically integrated moisture flux

divergence (shaded, mm/day) between Case_PD and Case_PI in JJA

We further analyze the difference of streamline and temperature difference at 10°E (Figure 2.5), from which we can see the cooling effect of sulfate aerosols from 400hPa to 150hPa over the region extending from 15°N to 30°N. The cooling effect from middle-to-high level increase the temperature contrast between surface and higher level, resulting in increased upper motion from lower level. The ascending air in the North induces a subsidence over 5°N to 15°N, well corresponding to the decreased precipitation over West Africa region. The increased temperature near surface is also caused by downward motion. Therefore, cooling in the middle level over North Africa eventually causes the descending vertically velocity and reduces the precipitation over Sahel region. Aerosol indirect effect in East Asia is similar to that in West Africa, which will not be further discussed in this chapter.
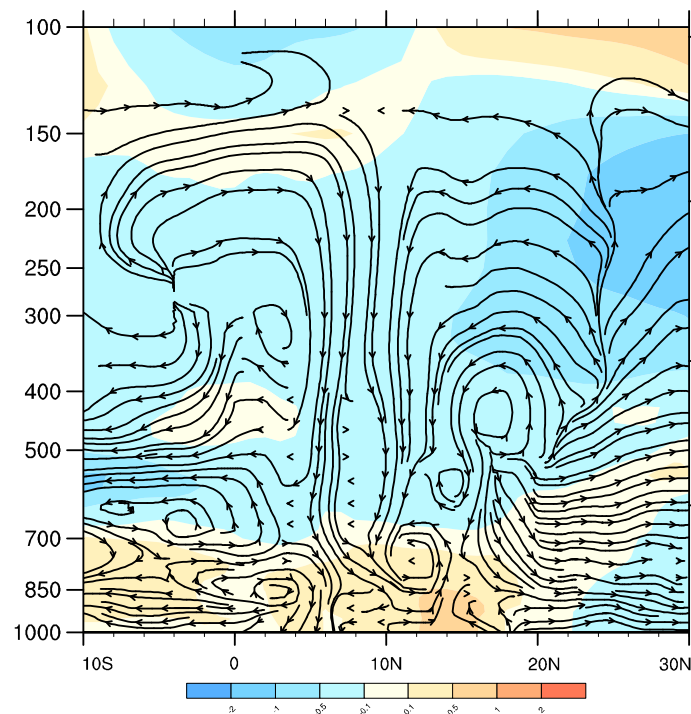
Figure 4.6 Latitude-height cross section of difference of streamline (v; −ω×1000) and

temperature (K, shaded) at 10°E between Case_PD and Case_PI in JJA

Chapter 5

# 5. Uncertainties and Conclusions

## 5.1 Uncertainties in estimating aerosol effects

Aerosol research has been carried on for several decades and a lot of progress has been made since 1970s (Twomey 1974, Charlson et al. 1992, Kiehl and Briegleb 1993). It has been widely acknowledged that aerosols exert negative radiative forcing globally, through both direct and indirect effects. Moreover, how aerosol influence surface temperature and precipitation in different monsoon systems through different effects still remains large uncertainties and is worth further analysis (Lau et al. 2016, Li et al. 2016).

One of the largest uncertainties lies in the direct effect of aerosols in WAM region. Although observational results suggest that the observed precipitation reduction in the WAM region is caused by the radiative effect of absorbing aerosols, its mechanism remains a mystery (Huang et al. 2009). Most studies agree on the two mechanisms mainly control the precipitation over WAM: the atmospheric heating component of absorption aerosols that enhances precipitation, and a surface cooling component that reduces precipitation (Miller and Tegen 1998, Yoshioka et al. 2007, Lau et al. 2009). Exactly how these two components play out depends on the model physics, and the ambient large-scale environment. In our study, the heating effect of dust plays a major part, which causes precipitation increase, while the surface cooling effect may not be well captured in our model.

This inherent complexity in ice nucleation processes makes aerosol indirect effect on ice clouds more unpredictable. Aerosols can act as ice nuclei (IN) by coming into contact with super-cooled cloud droplets (contact freezing) (Kärcher and Lohmann 2002), or by initiating freezing

from within a cloud droplet by immersion or condensation freezing (Hoose et al. 2010), or by acting as deposition nuclei (DeMott et al. 2003). The variety of aerosol-ice microphysical, dynamic, and thermodynamic interactions would involve large uncertainties in the parameterization of ice processes and require significant computational efforts. Inadequate understanding of the relative importance of these processes may induce large uncertainties in model simulations.

For liquid clouds, it is still not easy to reach agreement on quantifying, or even qualifying aerosol indirect effects on different variables such as precipitation and temperature even for those GCMs incorporating the same sulfate-Re relationship from Boucher and Lohmann (1995), (Ming et al. 2005). The divergences among different GCMs simulations are commonly induced by different cloud schemes such as cloud amount and microphysics scheme, auto-conversion parameterization, which are the core processes relating to aerosol-cloud interactions (Ramaswamy et al. 2001). Nonetheless, given a variety of differences among these studies in terms of GCM structure, cloud scheme and microphysics, and aerosol climatology, some agreement can be made, which shows some elements of the process are being captured well (Ming et al. 2005).

In the IPCC AR5, Boucher et al. (2013) have pointed out that "Clouds and aerosols continue to contribute the largest uncertainty to estimates and interpretations of the Earth's changing energy budget". The inherent complexity of aerosol-cloud interactions is the main reason inhibiting a better understanding and description of aerosol indirect effect. These processes have not been fully understood in cloud microphysical area, thus making it even harder to predict their behaviors in response to increasing aerosol loadings. Given the huge uncertainties estimating aerosol climate effect, Stevens (2013) proposed that: a better understanding of basic processes, such as how cloudiness and large-scale atmospheric circulation respond to warming/cooling, may help to make progress in quantifying the Earth's present and future climate change (Stevens 2013).

## 5.2 Conclusion

Our study carries out a series of climate simulations to investigate aerosol direct and indirect effect on both ice and liquid cloud. All experiments use GOCART data to represent aerosol distribution in present-day and has been conducted over a period spanning from Jan 1st, 2006 to Dec 31st, 2011 using WAMME II climatology SST. In the final part, we make some preliminary conclusions by comparing the relative importance of each component on both global and regional scales.
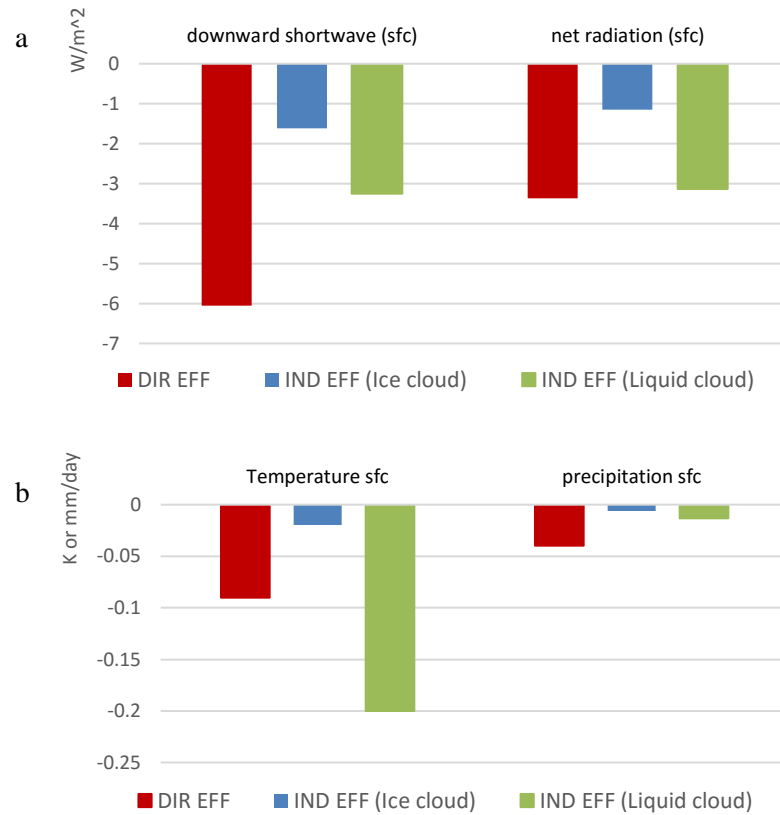


Figure 5.1 Aerosol direct and indirect effects on a) surface radiative budget b) surface temperature and precipitation averaged over the whole globe

Figure 5.1a shows the radiative forcing of aerosol direct and indirect effect on both ice clouds and liquid clouds, among which aerosol direct effect has the largest magnitude. The net radiation is relatively smaller than shortwave radiation because of positive longwave heating both either absorption aerosols or increased cloud cover. The indirect effect on liquid cloud seems to have smaller longwave feedback because most of them can be treated act as black bodies. A lot of regions show decreased land surface temperature resulting from aerosols, especially in higher latitude in North Hemisphere while the precipitations are less predictable. Aerosol indirect effects on averaged global precipitations are close to zero because the change of precipitation is heterogeneous in different regions.
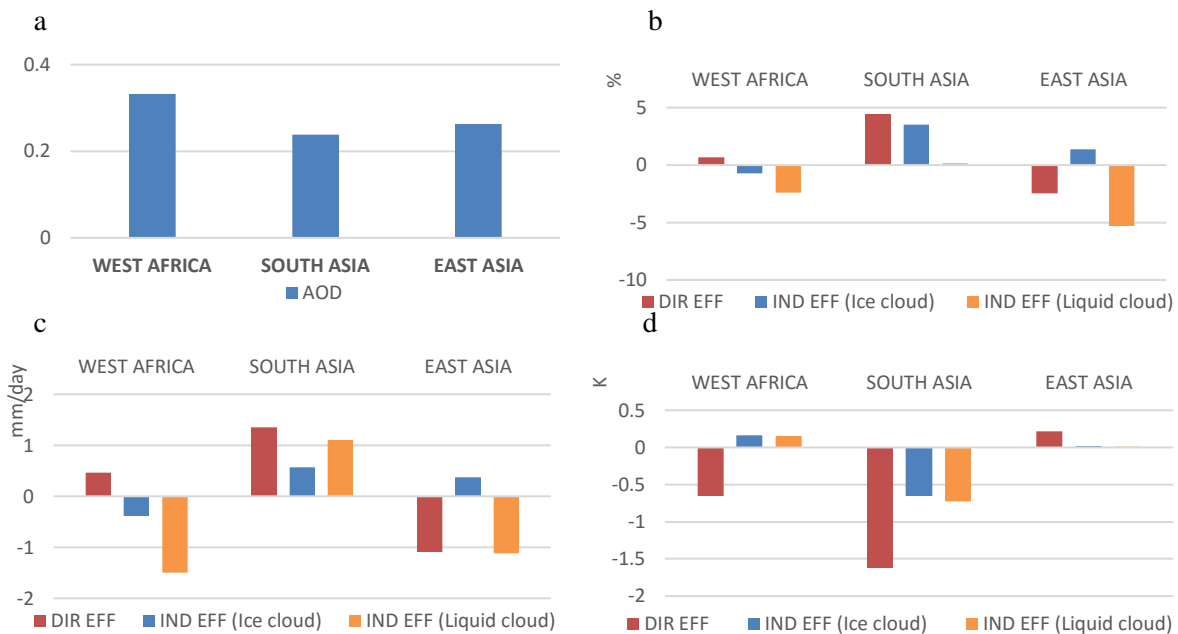


Figure 5.2a) Averaged AOD b) Aerosol effects on cloud fraction c) Aerosol effects on precipitation d) aerosol effects on precipitation in West Africa, South Asia and East Asia

Figure 5.1 shows the averaged AOD in West Africa, South Asia and East Asia, among which the AOD in West Africa is the largest (more than 0.3). Though the magnitude of AOD

seems similar in these monsoon regions, their climatic effects are quite different. Figure 5.2 b-d summarized the aerosol effects on regional climate. The direct effect of absorption aerosols in West Africa and South Asia caused precipitation increase exceeding 1mm/day because of the "elevated heat pump" mechanism while scattering aerosol like sulfate aerosol causes precipitation decrease over East Asia. The net radiative forcing of aerosol indirect effect on ice clouds is dependent on the relative magnitude of shortwave and longwave forcing and hence cause changes in vertical velocity. Precipitations is quite consistent with vertical velocity change. In South Asia and East Asia where net radiation increases, the upward motion is enhanced and results in precipitation increase. In West Africa, the situation is reversed. Aerosol indirect effect (liquid clouds) on precipitation is also consistent with net radiation change. The net radiation decrease over East Asia and West Africa correspond to the low-level descending motion. The change of precipitations will affect the partitioning between sensible heat, latent heat and ground heat flux, which further influences on surface temperature. The temperature changes mainly respond to temperature change and could be adjusted by precipitation increase and decrease as mentioned in Chapter 2.

REFERENCE:

Ackerman, A. S., O. B. Toon, D. E. Stevens, A. J. Heymsfield, V. Ramanathan and E. J. Welton (2000). "Reduction of tropical cloudiness by soot." *Science* **288**(5468): 1042-1047.

Albrecht, B. A. (1989). "Aerosols, Cloud Microphysics, and Fractional Cloudiness." *Science* **245**(4923): 1227-1230.

Boucher, O. and U. Lohmann (1995). "The Sulfate-Ccn-Cloud Albedo Effect - a Sensitivity Study with 2 General-Circulation Models." *Tellus Series B-Chemical and Physical Meteorology* **47**(3): 281-300.

Boucher, O., D. Randall, P. Artaxo, C. Bretherton, G. Feingold, P. Forster, . . . U. Lohmann (2013). Clouds and aerosols. Climate change 2013: The physical science basis. Contribution of working group I to the fifth assessment report of the intergovernmental panel on climate change, Cambridge University Press**:** 571-657.

Brenguier, J. L., H. Pawlowska, L. Schuller, R. Preusker, J. Fischer and Y. Fouquart (2000). "Radiative properties of boundary layer clouds: Droplet effective radius versus number concentration." *Journal of the Atmospheric Sciences* **57**(6): 803-821.

Charlson, R. J., S. E. Schwartz, J. M. Hales, R. D. Cess, J. A. Coakley, J. E. Hansen and D. J. Hofmann (1992). "Climate Forcing by Anthropogenic Aerosols." *Science* **255**(5043): 423-430.

Chin, M., P. Ginoux, S. Kinne, O. Torres, B. N. Holben, B. N. Duncan, . . . T. Nakajima (2002). "Tropospheric aerosol optical thickness from the GOCART model and comparisons with satellite and Sun photometer measurements." *Journal of the Atmospheric Sciences* **59**(3): 461-483.

Chou, M.-D., M. J. Suarez, C.-H. Ho, M. M.-H. Yan and K.-T. Lee (1998). "Parameterizations for Cloud Overlapping and Shortwave Single-Scattering Properties for Use in General Circulation and Cloud Ensemble Models." *Journal of Climate* **11**(2): 202-214.

Chuang, C. C., J. E. Penner, K. E. Taylor and J. J. Walton (1993). Climate effects of anthropogenic sulfate: Simulations from a coupled chemistry/climate model, ; Lawrence Livermore National Lab., CA (United States).

DeMott, P. J., K. Sassen, M. R. Poellot, D. Baumgardner, D. C. Rogers, S. D. Brooks, . . . S. M. Kreidenweis (2003). "African dust aerosols as atmospheric ice nuclei." *Geophysical Research Letters* **30**(14): n/a-n/a.

Diehl, K. and S. K. Mitra (1998). "A laboratory study of the effects of a kerosene-burner exhaust on ice nucleation and the evaporation rate of ice crystals." *Atmospheric Environment* **32**(18): 3145-3151.

Feingold, G., W. L. Eberhard, D. E. Veron and M. Previdi (2003). "First measurements of the Twomey indirect effect using ground-based remote sensors." *Geophysical Research Letters* **30**(6).

Fels, S. B. and M. D. Schwarzkopf (1975). "The simplified exchange approximation: A new method for radiative transfer calculations." *Journal of the Atmospheric Sciences* **32**(7): 1475-1488.

Gu, Y., J. Farrara, K. N. Liou and C. R. Mechoso (2003). "Parameterization of cloud-radiation processes in the UCLA general circulation model." *Journal of Climate* **16**(20): 3357-3370.

Gu, Y., K. N. Liou, J. H. Jiang, H. Su and X. Liu (2012). "Dust aerosol impact on North Africa climate: a GCM investigation of aerosol-cloud-radiation interactions using A-Train satellite data." *Atmospheric Chemistry and Physic*s **12**(4): 1667-1679.

Gu, Y., K. N. Liou, Y. Xue, C. R. Mechoso, W. Li and Y. Luo (2006). "Climatic effects of different aerosol types in China simulated by the UCLA general circulation model*." Journal of Geophysical Research* **111**(D15).

Gu, Y., Y. Xue, F. De Sales and K. N. Liou (2015). "A GCM investigation of dust aerosol impact on the regional climate of North Africa and South/East Asia." *Climate Dynamics* **46**(7-8): 2353-2370.

Hansen, J., M. Sato and R. Ruedy (1997). "Radiative forcing and climate response." *Journal of Geophysical Research-Atmospheres* **102**(D6): 6831-6864.

Haywood, J. and O. Boucher (2000). "Estimates of the direct and indirect radiative forcing due to tropospheric aerosols: A review." *Reviews of Geophysics* **38**(4): 513-543.

Hegg, D. A., R. J. Ferek and P. V. Hobbs (1993). "Light-Scattering and Cloud Condensation Nucleus Activity of Sulfate Aerosol Measured over the Northeast Atlantic-Ocean." *Journal of Geophysical Research-Atmospheres* **98**(D8): 14887-14894.

Ho, C. H., M. D. Chou, M. Suarez and K. M. Lau (1998). "Effect of ice cloud on GCM climate simulations." *Geophysical Research Letters* **25**(1): 71-74.

Hoose, C., J. E. Kristjansson and S. M. Burrows (2010). "How important is biological ice nucleation in clouds on a global scale?" *Environmental Research Letters* **5**(2).

Houghton, J. T. (1996). Climate change 1995: The science of climate change: contribution of working group I to the second assessment report of the Intergovernmental Panel on Climate Change, Cambridge University Press.

Huang, J. F., C. D. Zhang and J. M. Prospero (2009). "African aerosol and large-scale precipitation variability over West Africa." *Environmental Research Letters* **4**(1).

Jiang, H. L., H. W. Xue, A. Teller, G. Feingold and Z. Levin (2006). "Aerosol effects on the lifetime of shallow cumulus." *Geophysical Research Letters* **33**(14).

Jiang, J. H. and H. Su (2010). "Clean and polluted clouds: Relationships among pollution, ice cloud and precipitation in South America (vol 35, L10804 , 2008)." *Geophysical Research Letters* **37**.

Jiang, J. H., H. Su, C. Zhai, S. T. Massie, M. R. Schoeberl, P. R. Colarco, . . . K. N. Liou (2011). "Influence of convection and aerosol pollution on ice cloud particle effective radius." *Atmospheric Chemistry and Physics* **11**(2): 457-463.

Jiang, Y. Q., X. H. Liu, X. Q. Yang and M. H. Wang (2013). "A numerical study of the effect of different aerosol types on East Asian summer clouds and precipitation." *Atmospheric Environment* **70**: 51-63.

Jones, A., D. L. Roberts and A. Slingo (1994). "A Climate Model Study of Indirect Radiative Forcing by Anthropogenic Sulfate Aerosols." *Nature* **370**(6489): 450-453.

Kärcher, B., J. Hendricks and U. Lohmann (2006). "Physically based parameterization of cirrus cloud formation for use in global atmospheric models." *Journal of Geophysical Research- Atmospheres* **111**(D1): n/a-n/a.

Karcher, B. and U. Lohmann (2003). "A parameterization of cirrus cloud formation: Heterogeneous freezing." *Journal of Geophysical Research- Atmospheres* **108**(D14).

Kärcher, B. and U. Lohmann (2002). "A parameterization of cirrus cloud formation: Homogeneous freezing of supercooled aerosols." *Journal of Geophysical Research- Atmospheres* **107**(D2): AAC 4-1-AAC 4-10.

Kaufman, Y. J. and R. S. Fraser (1997). "The effect of smoke particles on clouds and climate forcing." *Science* **277**(5332): 1636-1639.

Kiehl, J. T. and B. P. Briegleb (1993). "The Relative Roles of Sulfate Aerosols and Greenhouse Gases in Climate Forcing." *Science* **260**(5106): 311-314.

Kiehl, J. T., T. L. Schneider, P. J. Rasch, M. C. Barth and J. Wong (2000). "Radiative forcing due to sulfate aerosols from simulations with the National Center for Atmospheric Research Community Climate Model, Version 3." *Journal of Geophysical Research-Atmospheres* **105**(D1): 1441-1457.

Kim, B. G., M. A. Miller, S. E. Schwartz, Y. G. Liu and Q. L. Min (2008). "The role of adiabaticity in the aerosol first indirect effect." Journal of Geophysical Research-Atmospheres **113**(D5).

Koepke, P., M. Hess, I. Schult and E. Shettle (1997). "Global aerosol data set." *MPI Meteorologie Hamburg Rep* **243**: 44.

Kristjansson, J. E., T. Iversen, A. Kirkevag, O. Seland and J. Debernard (2005). "Response of the climate system to aerosol direct and indirect forcing: Role of cloud feedbacks." *Journal of Geophysical Research-Atmospheres* **110**(D24).

L'Ecuyer, T. S. and J. H. Jiang (2010). "Touring the atmosphere aboard the A-Train." *Physics Today* **63**(7): 36-41.

Langner, J. and H. Rodhe (1991). "A global three-dimensional model of the tropospheric sulfur cycle." *Journal of Atmospheric Chemistry* **13**(3): 225-263.

Lau, K. M. and K. M. Kim (2006). "Observational relationships between aerosol and Asian monsoon rainfall, and circulation." *Geophysical Research Letters* **33**(21).

Lau, K. M., K. M. Kim, Y. C. Sud and G. K. Walker (2009). "A GCM study of the response of the atmospheric water cycle of West Africa and the Atlantic to Saharan dust radiative forcing." *Annales Geophysicae* **27**(10): 4023-4037.

Lau, K. M., M. K. Kim and K. M. Kim (2006). "Asian summer monsoon anomalies induced by aerosol direct forcing: the role of the Tibetan Plateau." *Climate Dynamics* **26**(7-8): 855-864.

Lau, W. K. M., K.-M. Kim, J.-J. Shi, T. Matsui, M. Chin, Q. Tan, . . . W. K. Tao (2016). "Impacts of aerosol–monsoon interaction on rainfall and circulation over Northern India and the Himalaya Foothills." *Climate Dynamics*: 1-16.

Lee, K. H., Z. Q. Li, M. S. Wong, J. Y. Xin, Y. S. Wang, W. M. Hao and F. S. Zhao (2007). "Aerosol single scattering albedo estimated across China from a combination of ground and satellite measurements." *Journal of Geophysical Research-Atmospheres* **112**(D22).

Lee, S. S., G. Feingold and P. Y. Chuang (2012). "Effect of Aerosol on Cloud-Environment Interactions in Trade Cumulus." Journal of the Atmospheric Sciences **69**(12): 3607-3632.

Li, S., T. Wang, F. Solmon, B. Zhuang, H. Wu, M. Xie, . . . X. Wang (2016). "Impact of aerosols on regional climate in southern and northern China during strong/weak East Asian summer monsoon years." *Journal of Geophysical Research- Atmospheres* **121**(8): 4069-4081.

Li, Z. Q., W. K. M. Lau, V. Ramanathan, G. Wu, Y. Ding, M. G. Manoj, . . . G. P. Brasseur (2016). "Aerosol and monsoon climate interactions over Asia." *Reviews of Geophysics* 54(4): 866-929.

Lohmann, U. and J. Feichter (1997). "Impact of sulfate aerosols on albedo and lifetime of clouds: A sensitivity study with the ECHAM4 GCM." *Journal of Geophysical Research-Atmosphere*s **102**(D12): 13685-13700.

Lohmann, U. and E. Roeckner (1996). "Design and performance of a new cloud microphysics scheme developed for the ECHAM general circulation model." *Climate Dynamics* **12**(8): 557-572.

Menon, S., J. Hansen, L. Nazarenko and Y. Luo (2002). "Climate effects of black carbon aerosols in China and India." *Science* **297**(5590): 2250-2253.

Miller, R. L. and I. Tegen (1998). "Climate response to soil dust aerosols." *Journal of Climate* **11**(12): 3247-3267.

Ming, Y., V. Ramaswamy, P. A. Ginoux, L. W. Horowitz and L. M. Russell (2005). "Geophysical Fluid Dynamics Laboratory general circulation model investigation of the indirect radiative effects of anthropogenic sulfate aerosol." *Journal of Geophysical Research- Atmospheres* **110**(D22).

Myhre, G., D. Shindell, F.-M. Bréon, W. Collins, J. Fuglestvedt, J. Huang, . . . B. Mendoza (2013). "Anthropogenic and natural radiative forcing." Climate change **423**.

Penner, J. E., C. C. Chuang and K. Grant (1998). "Climate forcing by carbonaceous and sulfate aerosols." *Climate Dynamics* **14**(12): 839-851.

Pincus, R. and M. B. Baker (1994). "Effect of Precipitation on the Albedo Susceptibility of Clouds in the Marine Boundary-Layer." *Nature* **372**(6503): 250-252.

Qian, Y., H. P. Yan, Z. S. Hou, G. Johannesson, S. Klein, D. Lucas, . . . C. Zhao (2015). "Parametric sensitivity analysis of precipitation at global and local scales in the

Community Atmosphere Model CAM5." *Journal of Advances in Modeling Earth Systems* **7**(2): 382-411.

Ramanathan, V. and Y. Feng (2009). "Air pollution, greenhouse gases and climate change: Global and regional perspectives." *Atmospheric Environment* **43**(1): 37-50.

Ramaswamy, V., O. Boucher, J. Haigh, D. Hauglustaine, J. Haywood, G. Myhre, . . . F. Joos (2001). Radiative Forcing of Climate Change, Houghton, J. T. et al; Cambridge University Press, New York, NY, United States(US).; Pacific Northwest National Laboratory (PNNL), Richland, WA (US).

Rotstayn, L. D. (1999). "Indirect forcing by anthropogenic aerosols: A global climate model calculation of the effective-radius and cloud-lifetime effects." *Journal of Geophysical Research- Atmospheres* **104**(D8): 9369-9380.

Schwarzkopf, M. D. and S. B. Fels (1991). "The simplified exchange method revisited: An accurate, rapid method for computation of infrared cooling rates and fluxes." *Journal of Geophysical Research- Atmospheres* **96**(D5): 9075-9096.

Stevens, B. (2013). "CLIMATE SCIENCE Uncertain then, irrelevant now." *Nature* **503**(7474): 47-48.

Sundqvist, H., E. Berge and J. E. Kristjansson (1989). "Condensation and Cloud Parameterization Studies with a Mesoscale Numerical Weather Prediction Model." *Monthly Weather Review* **117**(8): 1641-1657.

Twomey, S. (1974). "Pollution and Planetary Albedo." *Atmospheric Environment* **8**(12): 1251-1256.

Wu, L. T., H. Su and J. H. Jiang (2013). "Regional simulation of aerosol impacts on precipitation during the East Asian summer monsoon." *Journal of Geophysical Research-Atmospheres* **118**(12): 6454-6467.

Xu, K. M. and D. A. Randall (1996). "A semiempirical cloudiness parameterization for use in climate models." *Journal of the Atmospheric Sciences* **53**(21): 3084-3102.

Xu, Q. (2001). "Abrupt change of the mid-summer climate in central east China by the influence of atmospheric pollution." *Atmospheric Environment* **35**(30): 5029-5040.

Xue, Y., F. De Sales, W. K. M. Lau, A. Boone, K.-M. Kim, C. R. Mechoso, . . . Z. Zhang (2016). "West African monsoon decadal variability and surface-related forcings: second West African Monsoon Modeling and Evaluation Project Experiment (WAMME II)." *Climate Dynamics* **47**(11): 3517-3545.

Xue, Y., H. M. H. Juang, W. P. Li, S. Prince, R. DeFries, Y. Jiao and R. Vasic (2004). "Role of land surface processes in monsoon development: East Asia and West Africa." *Journal of Geophysical Research- Atmospheres* **109**(D3): n/a-n/a.

Xue, Y., P. J. Sellers, J. L. Kinter and J. Shukla (1991). "A Simplified Biosphere Model for Global Climate Studies." *Journal of Climate* **4**(3): 345-364.

Xue, Y. K., F. De Sales, R. Vasic, C. R. Mechoso, A. Arakawa and S. Prince (2010). "Global and Seasonal Assessment of Interactions between Climate and Vegetation Biophysical Processes: A GCM Study with Different Land-Vegetation Representations." *Journal of Climate* **23**(6): 1411-1433.

Yoshioka, M., N. M. Mahowald, A. J. Conley, W. D. Collins, D. W. Fillmore, C. S. Zender and D. B. Coleman (2007). "Impact of desert dust radiative forcing on Sahel precipitation:

Relative importance of dust compared to sea surface temperature variations, vegetation changes, and greenhouse gas warming." *Journal of Climate* **20**(8): 1445-1467.

Zhan, X. W., Y. K. Xue and G. J. Collatz (2003). "An analytical approach for estimating CO2 and heat fluxes over the Amazonian region." *Ecological Modelling* **162**(1-2): 97-117.

Zhang, L., Q. B. Li, Y. Gu, K. N. Liou and B. Meland (2013). "Dust vertical profile impact on global radiative forcing estimation using a coupled chemical-transport-radiative-transfer model." *Atmospheric Chemistry and Physics* **13**(14): 7097-7114.

Zhang, Q., J. Meng, J. Quan, Y. Gao, D. Zhao, P. Chen and H. He (2012). "Impact of aerosol composition on cloud condensation nuclei activity." *Atmospheric Chemistry and Physics* **12**(8): 3783-3790.

Zhao, Q. Y. and F. H. Carr (1997). "A prognostic cloud scheme for operational NWP models." *Monthly Weather Review* **125**(8): 1931-1953.